Ocean Turbulence and Global Climate Variability:

Computational Mathematics for a (Very) Complex System

Richard Peltier
Department of Physics
University of Toronto

Global Climate Models are tuned to enable them to replicate modern climate dynamical observations

A Global Climate Model Cartoon

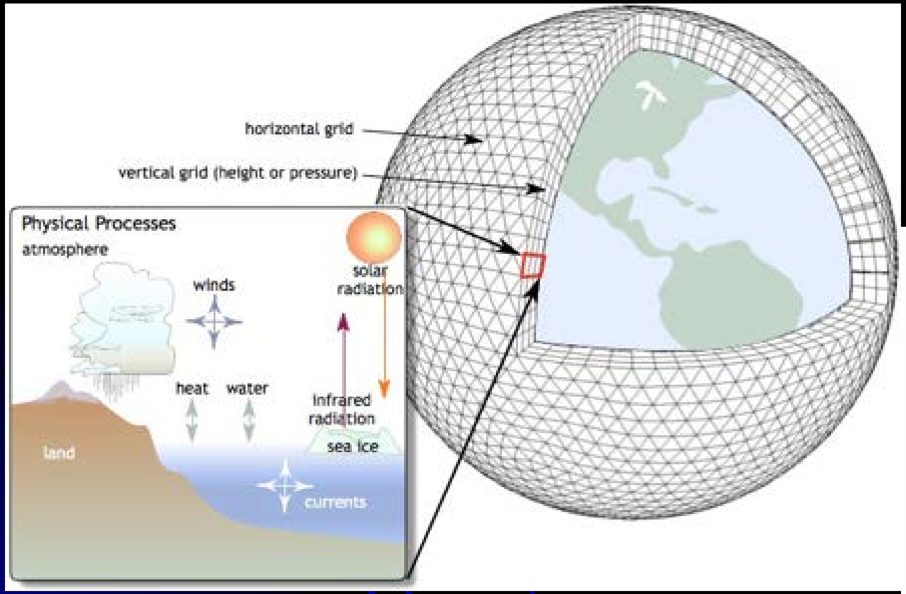

Imaging evolving atmospheric water vapor & rain

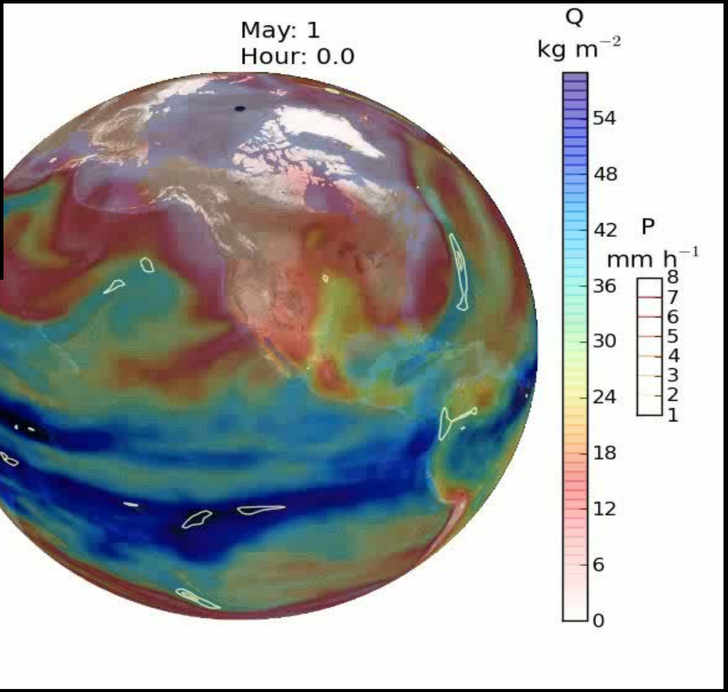

It has remained an issue as to whether such models have skill out side of the volume of parameter space in which they are tuned

Atmosphere-Land and Ocean- Sea Ice grids

Atmosphere-Land
Fast Physics

Ocean-Sea Ice
Slow Physics

NCAR CESM1

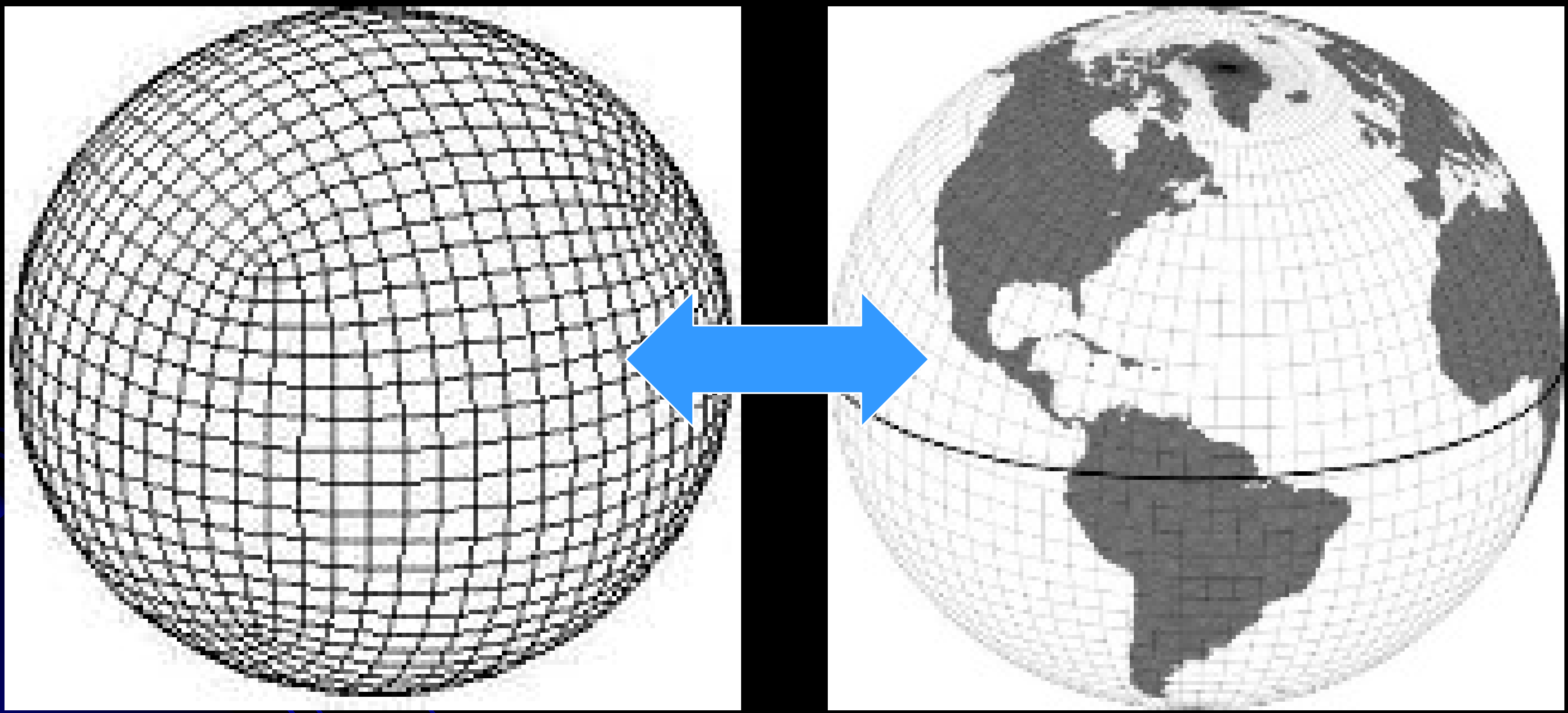

Control Volume Cubed sphere atmosphere-land 0.9 x 1.25 degree res, 0.25 deg latitudinally at the equator, 26 levels in the atmosphere

Spherical polar orthogonal grid In rotated co-ordinates, 1 x 1 degree resolution, 60 levels

Do these models have skill under climate conditions that differ radically from modern?

A period of Earth history during which a radically different climate regime prevailed was during the last glacial cycle of the Late Quaternary Ice-Age

60,000 -30,00 years ago

GRIP and NGRIP Summit Greenland Ice Cores: Relaxation oscillations of the global ocean circulation?

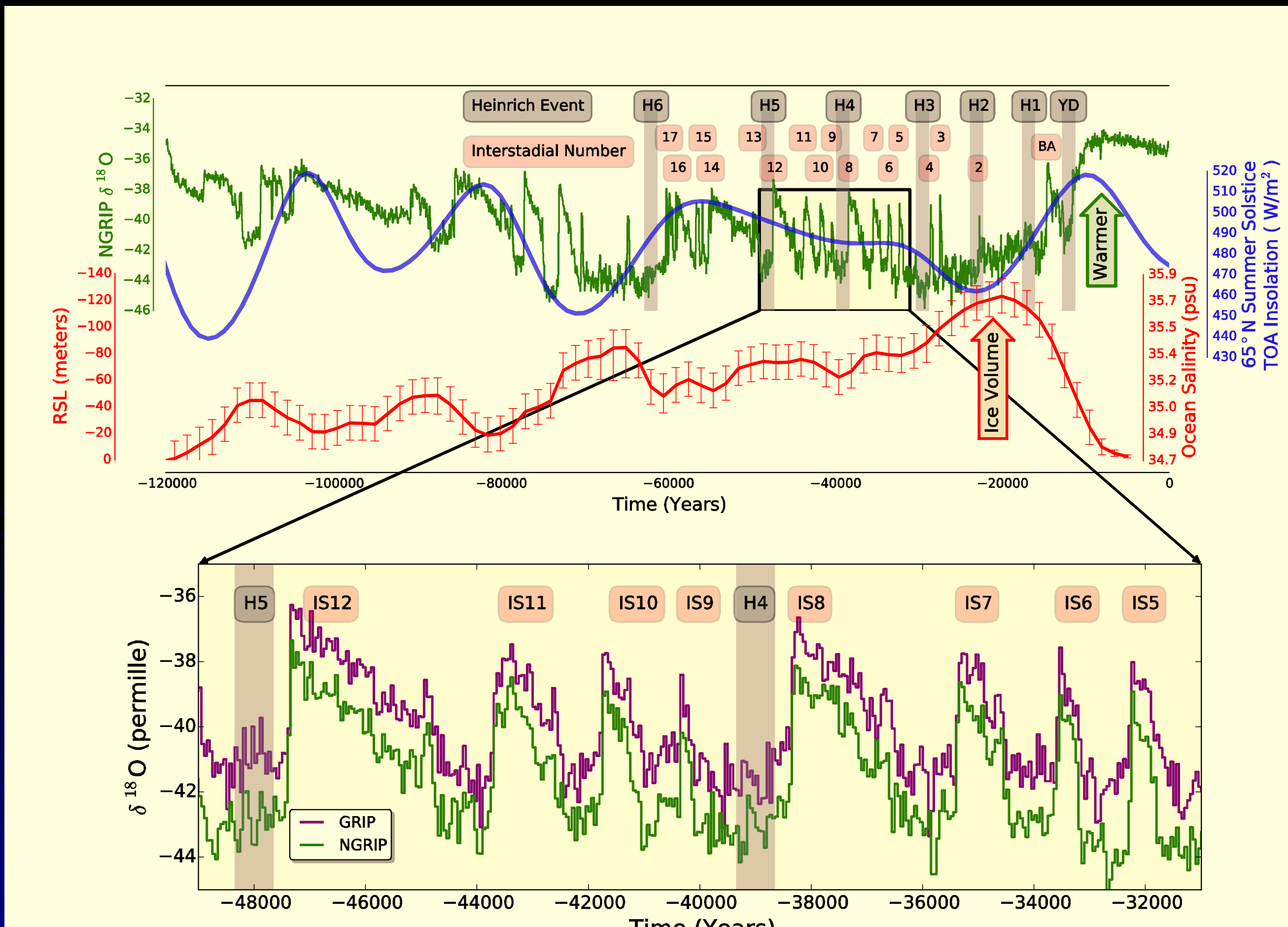

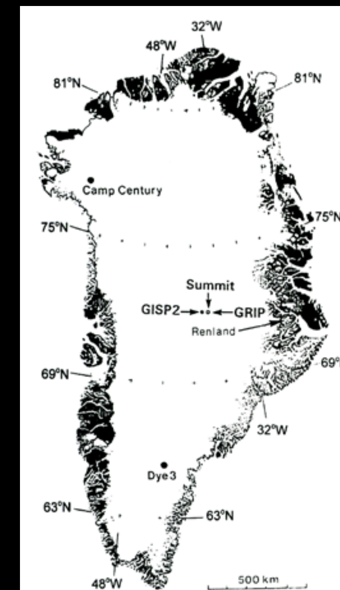

The oxygen isotopic ratio measured in ice is a measure of the temperature of the air from which precip. is derived.

Heinrich events (H) correspond to episodes during which intense instabilities occur on the eastern flank of the Laurentide ice sheet.

Outline

- Motivation: Past climate tests of climate model veracity—do modern coupled climate models have any significant skill in explaining climate dynamical behavior beyond the region of parameter space in which they have been tuned? The Dansgaard-Oeschger oscillation as a test
- The meridional overturning circulation (MOC) of the oceans and the nature of the stratified turbulence that is required to support it. The KH ansatz
- The Dansgaard-Oeschger Oscillation: glacial boundary conditions and solution of the initial value problem for glacial climate time dependence. A comprehensive model recovers the phenomenon as a “kicked” salt oscillator in which individual pulses have relaxation oscillation form
- Rapid climate change and D-O physics: the fast timescale of the relaxation oscillation is governed by the onset of intense thermohaline convective turbulence which opens a massive Polynya in the glacial sea ice lid and enables a warming transition which, in the model, occurs during a single winter season
- Summary

The Atlantic THC: Ocean Ventilation & the Meridional Overturning Circulation (MOC)

Surface Heat, Moisture and Buoyancy Fluxes

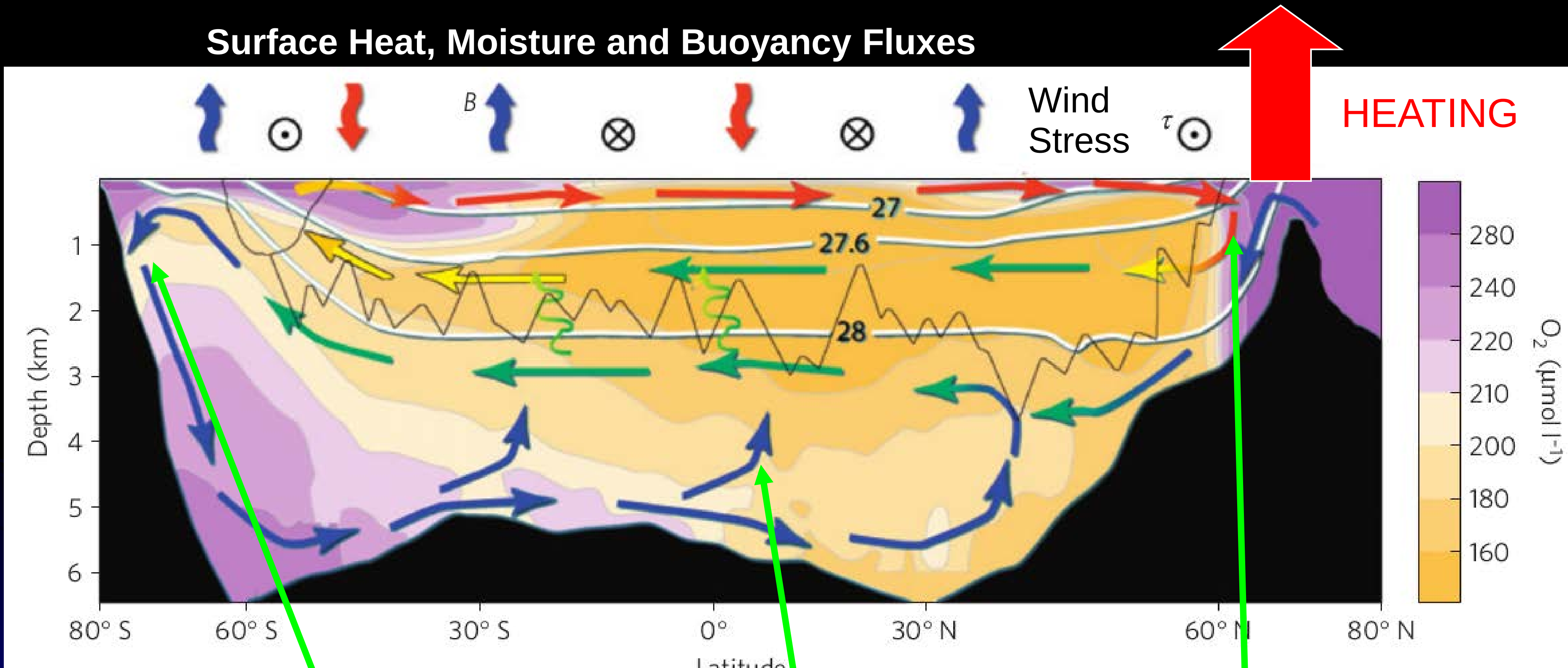

Antarctic Bottom Water Formation

Vertical Mixing

North Atlantic Deep Water Formation

Cartoon from Marshall and Speer, Nature Geoscience 2012

The Meridional Overturning Circulation (MOC) of the Oceans
and the stratified turbulence that supports it

Applicability of the KH Ansatz for the inference of diapycnal diffusivity

Parameterizations of these diffusivities are evolving rapidly: We show that the D-O oscillation process is small scale mixing dependent and therefor may be invoked to help constrain such parameterizations

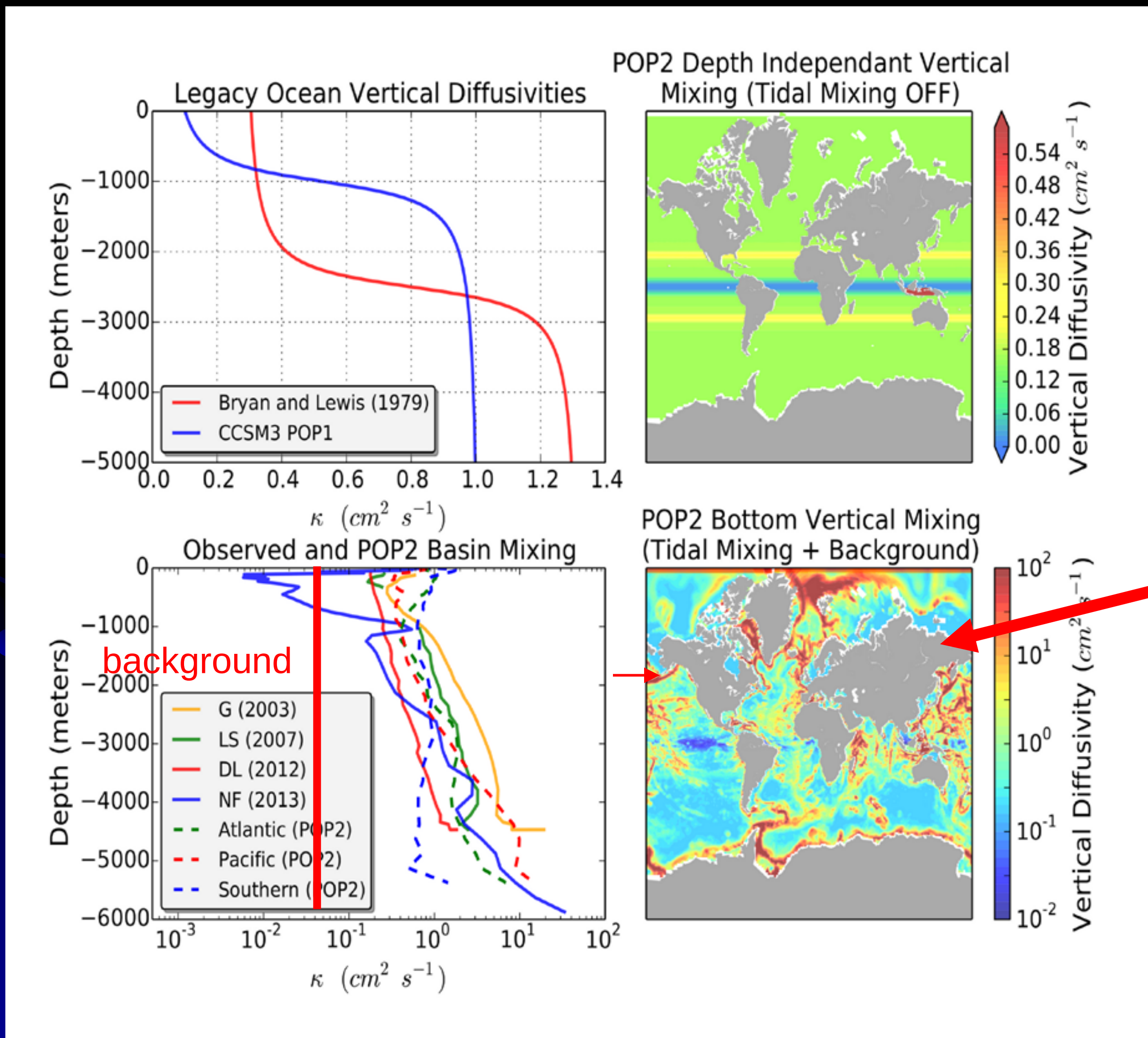

Our interest is in the question of the dependence of coupled climate model predictions of the D-O oscillation upon the parameterization of the vertical diapycnal diffusion of mass

A modern diffusivity map based upon the assumption that this turbulent process is controlled by dissipation of the “internal tide “

From P & Vettoretti GRL, 2014

Before considering the characteristics of the MOC under full glacial conditions and at high spatial and temporal resolution it is useful to establish the nature of the steady states as a function of surface boundary conditions and the strength of high latitude freshwater forcing conditions at low resolution. The following results were obtained using the CCSM3 version of the NCAR model.

Modern, Y-D and LGM SurfaceConditions:
Y-D=Younger Dryas; LGM=Last Glacial Maximum

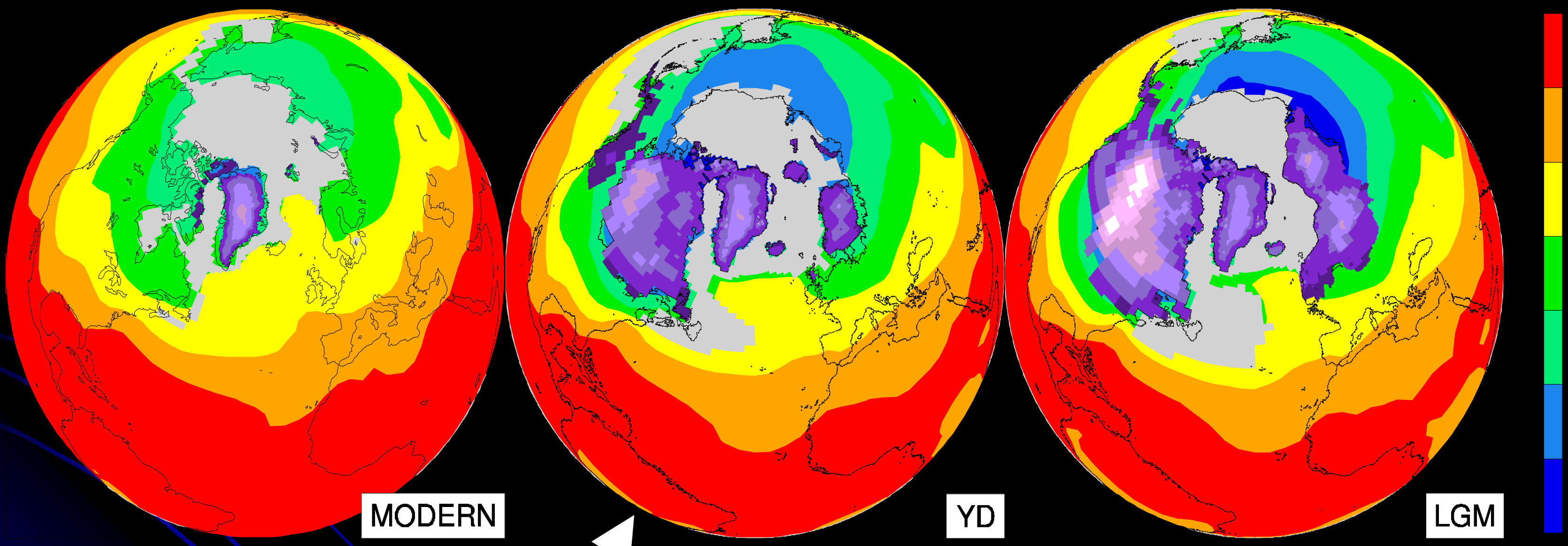

Note: at Y-D onset surface conditions
Were much closer to LGM than to modern

MOC Impacts Relative to the Controls: steady states as a function of anomalous freshwater forcing

Arctic Atlantic Arctic Atlantic

.1Sv

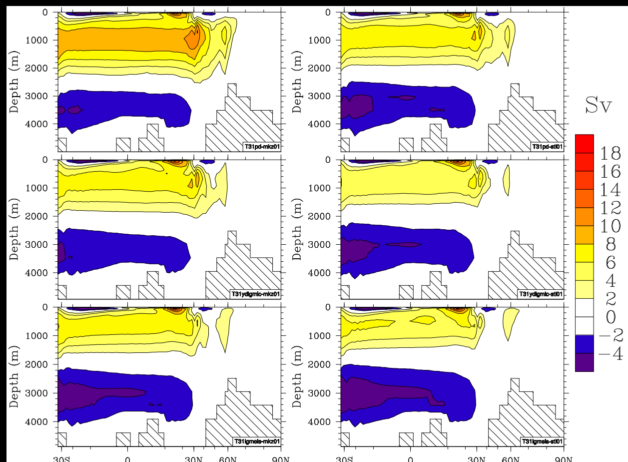

PD

YD

LGM

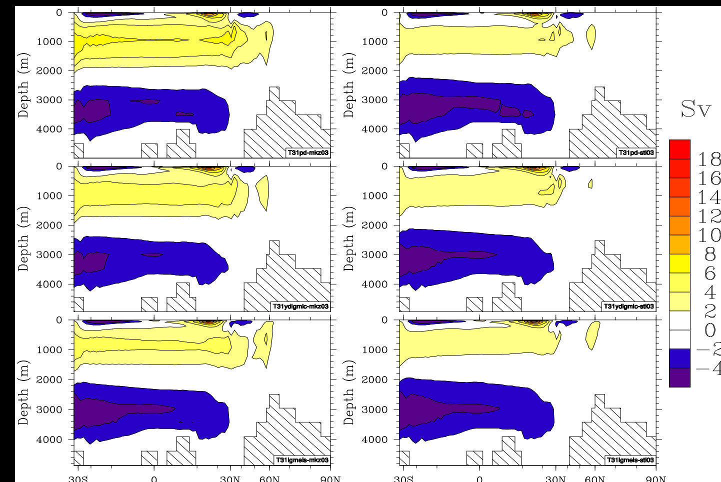

.3Sv

.2Sv

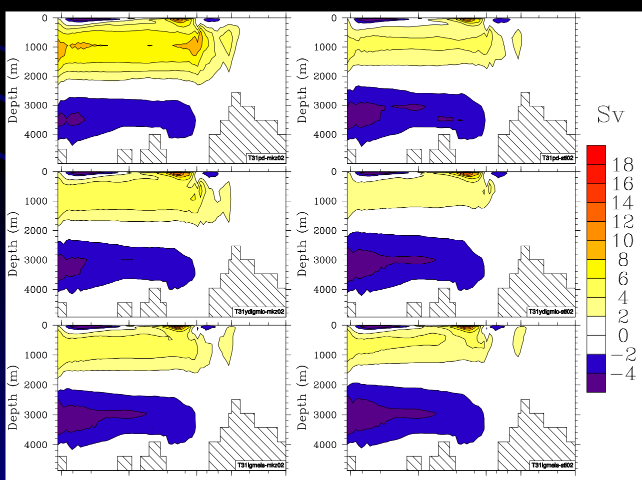

PD

YD

LGM

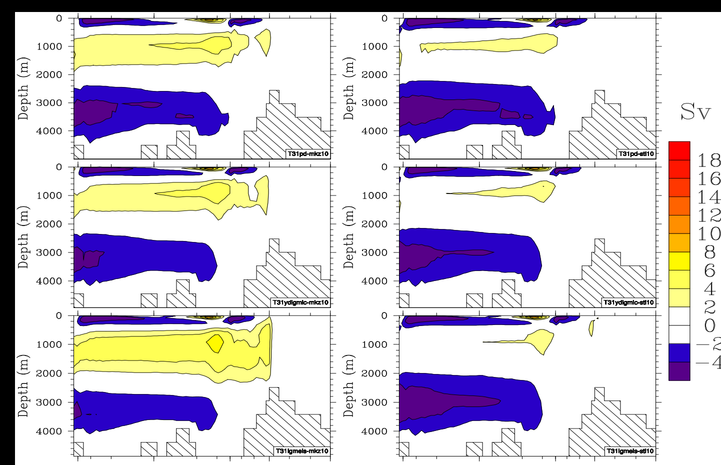

1.Sv

An example of a very high resolution simulation of a turbulent diapycnal mixing event due to breaking of a nonlinear Kelvin-Helmholtz wave at Re=6000 and Pr =8. DNS calculation using 60,0000 cores on the Toronto BGQ system. THE EVOLVING DENSITY FIELD

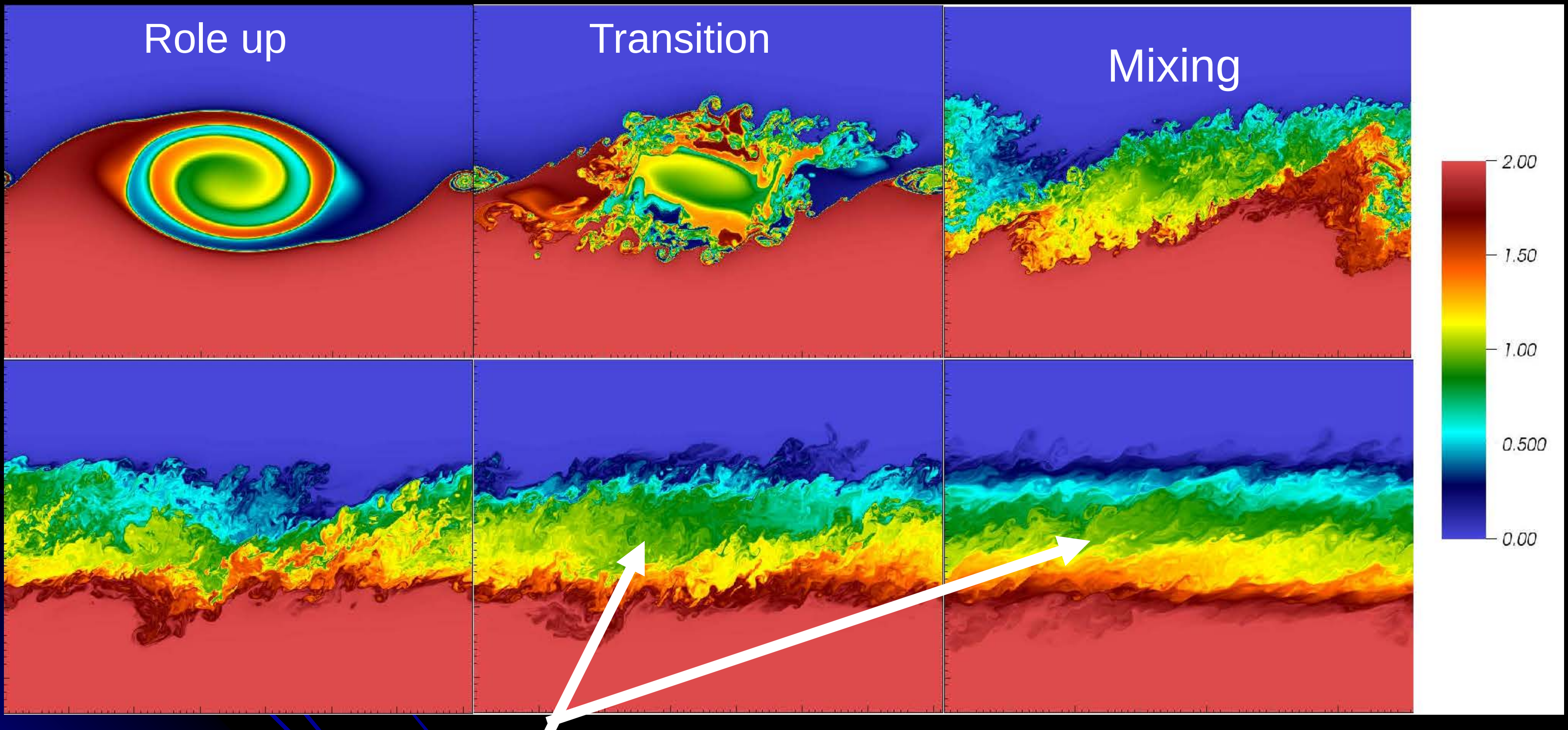

In the regime of fully developed 3-dimensional turbulent flow The turbulence acts to support a vertical flux of mass through the combined action of buoyancy flux and an additional process related to the anisotropy of the turbulence.

From Salehipour & P, JFM, 2015.

Holmboe waves also break at high Re to produce intense stratified turbulence

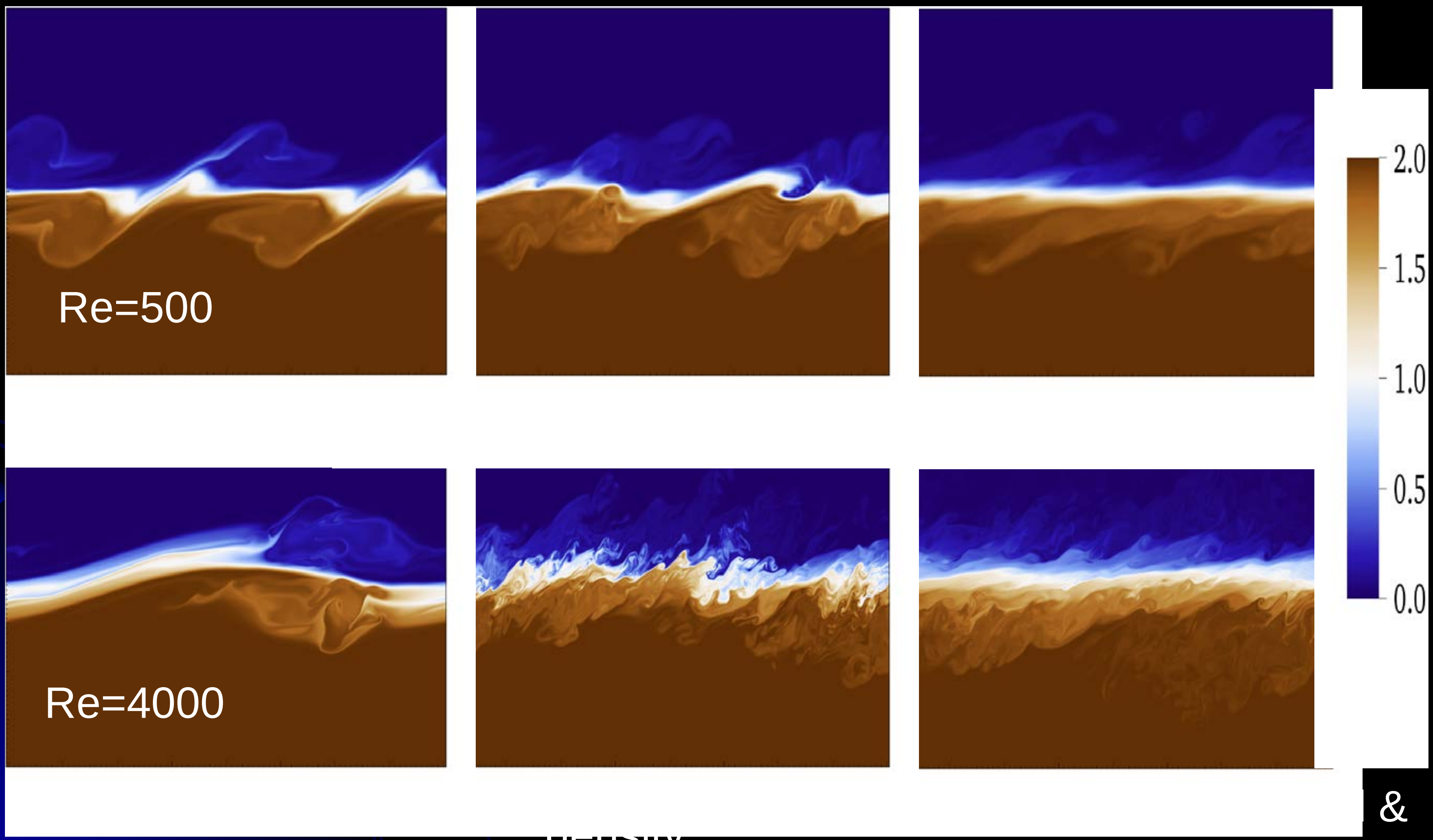

&

density

P JFM, 2016

Comparing free stratified shear driven turbulent diffusivities derived from the turbulent collapse of either Kelvin-Helmholtz or Holmboe waves

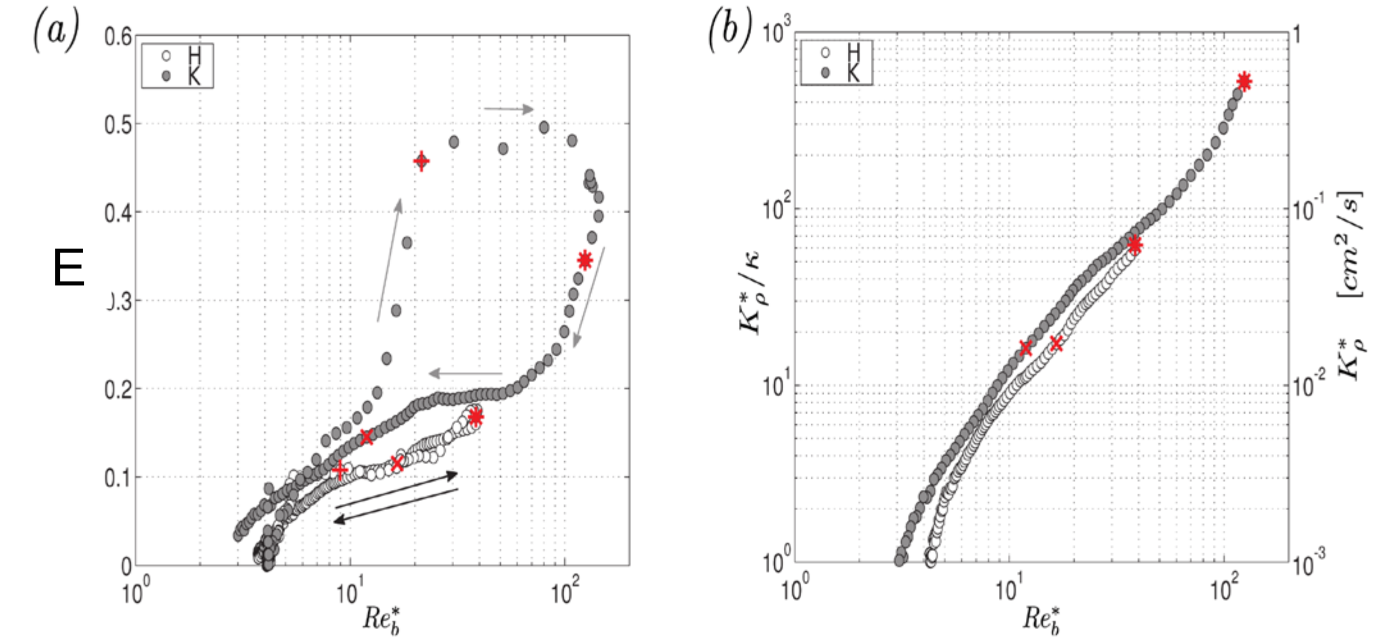

FIGURE 11. (Colour online) Variation with Re_b^* for simulation 'H' (white circles) and simulation 'K' (grey circles) of: (*a*) the irreversible mixing efficiency, η, as defined in (2.27) for the entire life cycle of HWI and KHI; and (*b*) the irreversible diapycnal diffusivity, K_ρ^*, as defined in (2.24) for $t \geqslant t_{3d}$. The data corresponding to times t_{2d} (marked by '+'), t_{3d} (marked by '$*$') and $t = t_{2d} + 100$ (marked by '$\times$') are also indicated. The direction of time evolution is also indicated by arrows in panel (*a*).

Salehipour, Caulfield & P, JFM, 2016

KH Ansatz fit to stratified ocean turbulence observations

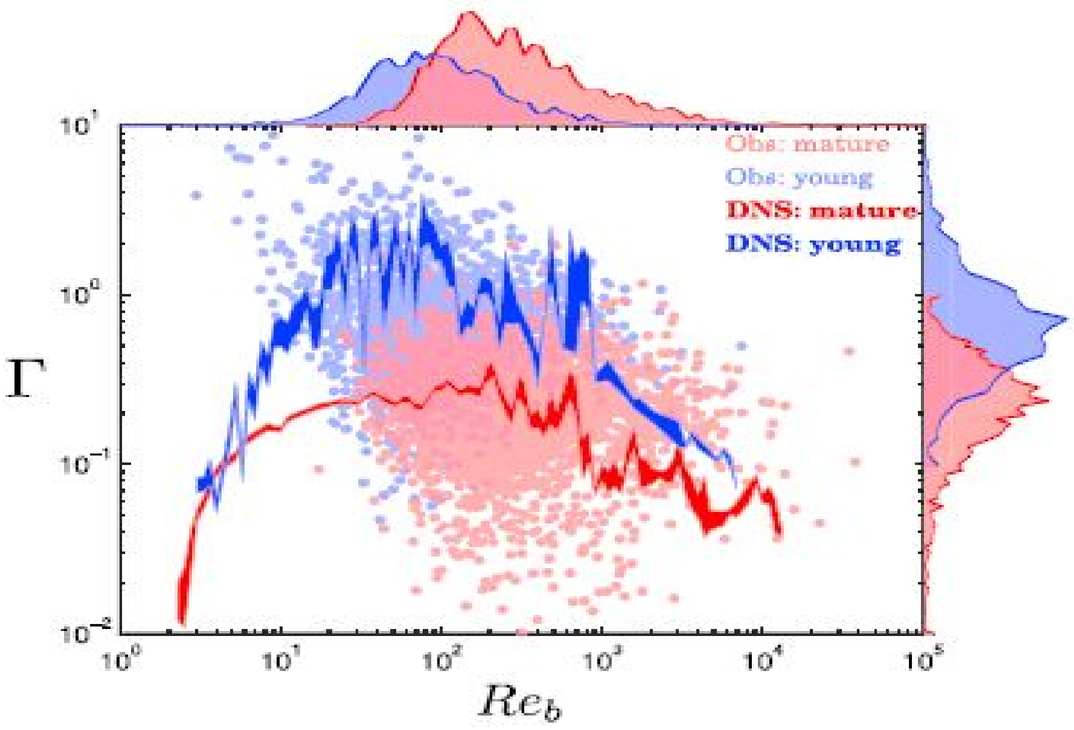

Figure 2. Re_b dependence of Γ, comparing the young and mature mixing events obtained from oceanic measurements of *Smyth et al.* [2001] (see *Moum* [1996] and *Lien et al.* [1995] for source of data) and an extensive suite of DNS analyses associated with the growth, turbulent breakdown, and decay of a Kelvin-Helmholtz instability (i.e., KH-ansatz) taken from *Salehipour and Peltier* [2015]. The histograms on both abscissa and ordinate illustrate the distribution of these mixing events in field observations. The DNS data sets are also binned for clarity of presentation.

See Salehipour et al 2016 GRL and Mashayek, Salehipour et al GRL 2017 For explicit discussions of the parameterizations that are supported by the DNS data

GRIP and NGRIP Summit Greenland Ice Cores: Relaxation oscillations of the global ocean circulation?

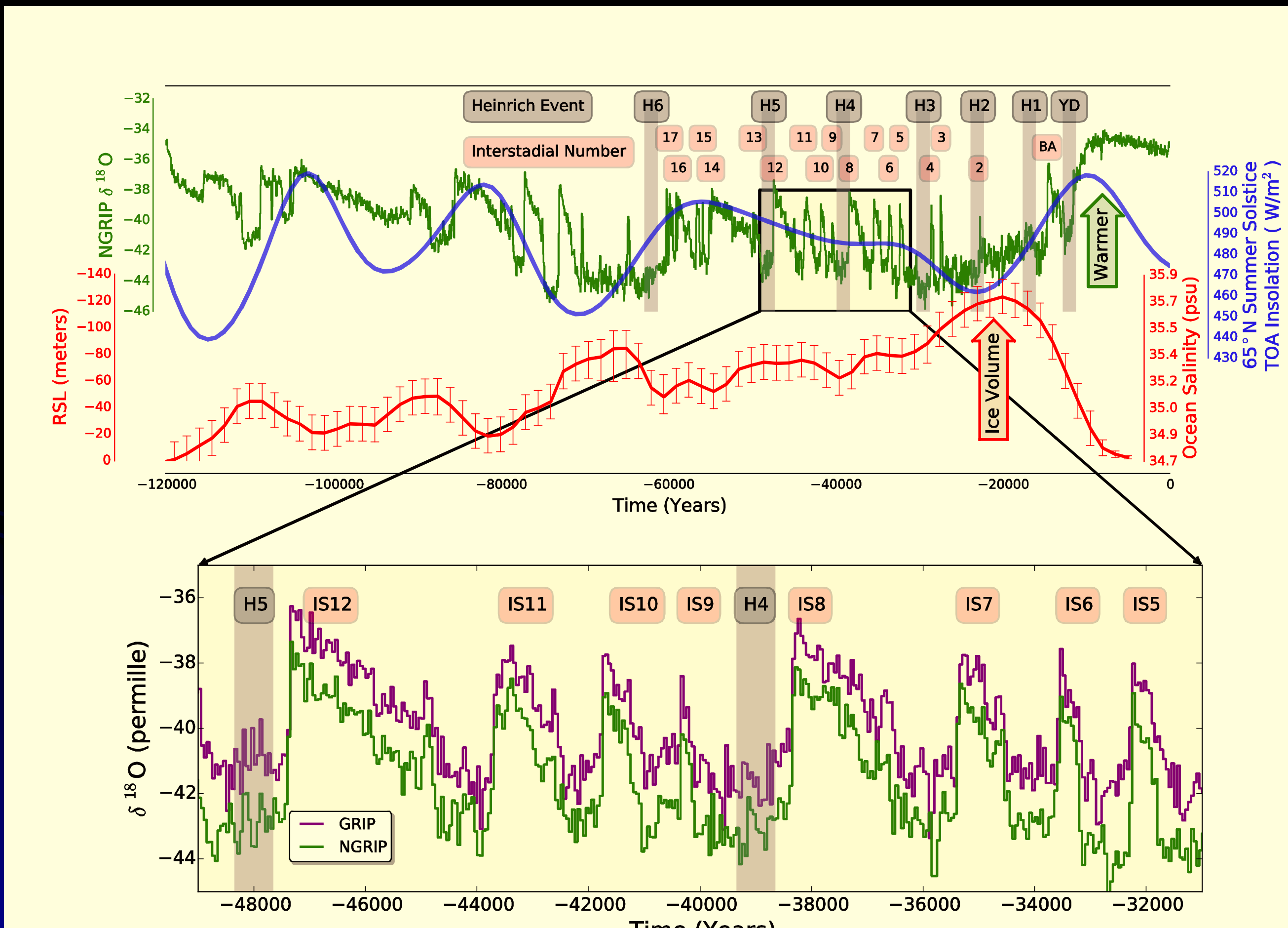

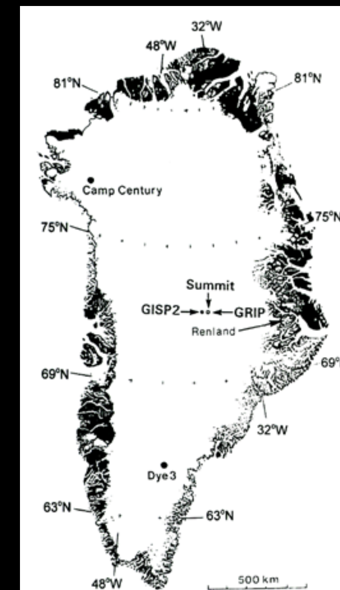

The oxygen isotopic ratio measured in ice is a measure of the temperature of the air from which precip. is derived.

Heinrich events (H) correspond to episodes during which intense instabilities occur on the eastern flank of the Laurentide ice sheet.

Ice-Age Boundary Conditions: how do we infer them?

Models of Glaciation History---ICE-6G_C (VM5a)

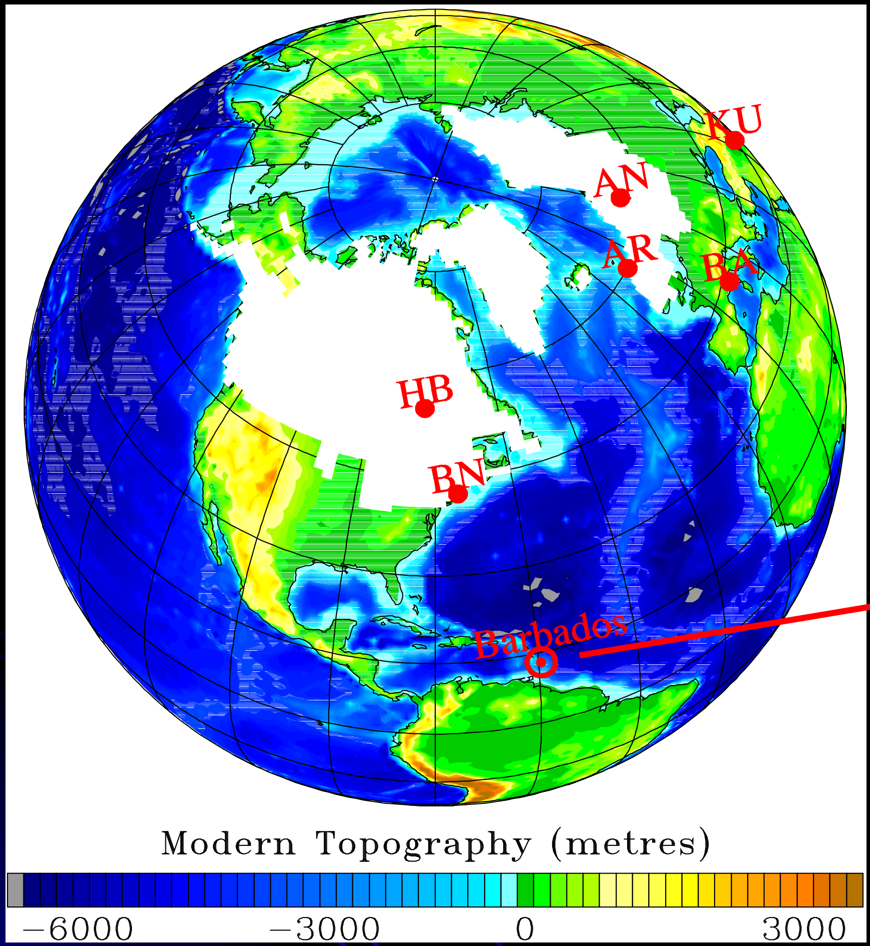

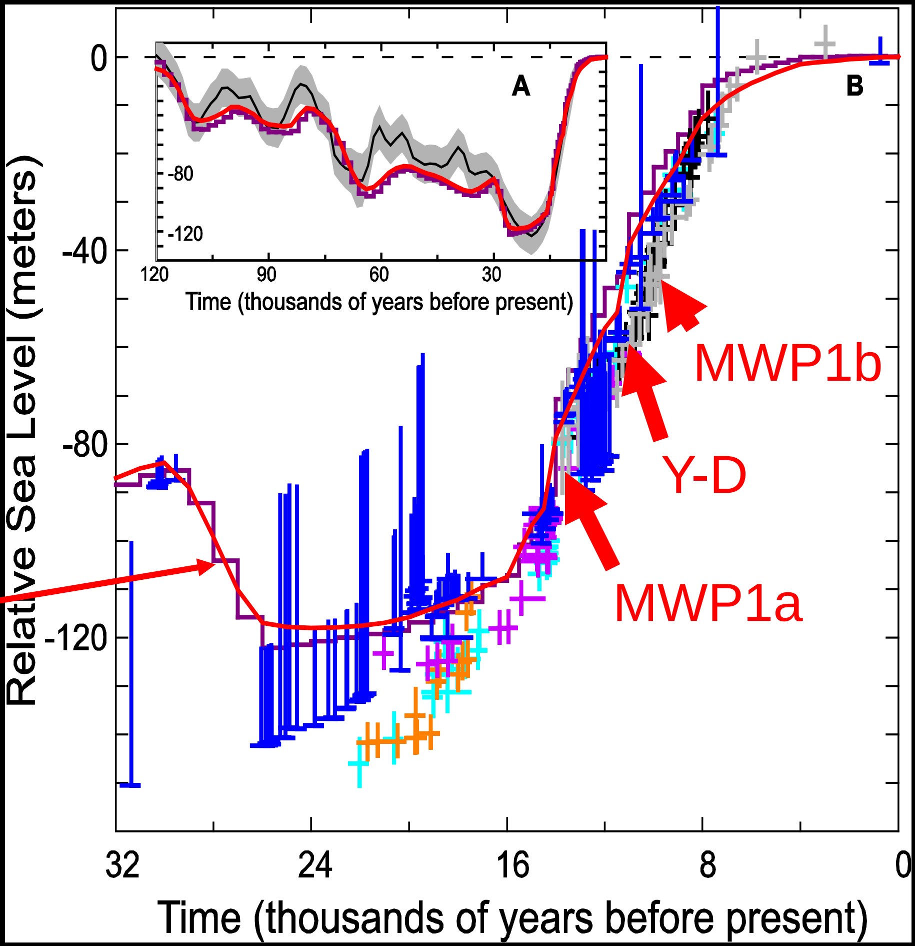

NOTE: these figures are from the recent paper by Peltier and Fairbanks that appeared in the December 2006 issue of QSR (25, 3322-3337). The new Barbados RSL curve appeared in the Working Group 1 Report of the IPCC AR4

Origins

Sea Level Equations: With and Without Rotational Feedback

R-Peltier 1974
G-Peltier &Andrews1976
DPhi/g-Farrell and Clark 1976
S-Peltier et al, 1978 &Clark et al, 1978

Omega-I, Peltier,1982
Wu and Peltier, 1984

C-Peltier 1994

The Formal Theory of Glacial Isostatic Adjustment

The variation of relative sea level forced by the glaciation - deglaciation process is determined by the Sea Level Equation. With $S(\theta,\lambda,t)$ the history of relative sea level, then :

$$S(\theta,\lambda,t)=C(\theta,\lambda,t)\left[G(\theta,\lambda,t)-R(\theta,\lambda,t)\right]$$
$$=C(\theta,\lambda,t)\left[\int_{-\infty}^{t}\int_{\Omega}\int L(\theta',\lambda',t')\cdot\left\{\frac{\phi(\gamma,t-t')}{g}-\Gamma(\gamma,t-t')\right\}d\Omega' dt'+\frac{\Delta\Phi(t)}{g}\right]$$

The history of surface loading $L(\theta,\lambda,t)$ may be expanded as :

$$L(\theta,\lambda,t)=\rho_I I(\theta,\lambda,t)+\rho_W S(\theta,\lambda,t)$$

And the Green Functions ϕ & Γ have expansions :

$$\phi(\overbrace{\theta,\lambda}^{\gamma},t)=\frac{a g}{m_e}\sum_{l=0}^{\infty}k_\ell P_\ell(\cos\gamma)$$
$$\Gamma(\overbrace{\theta,\lambda}^{\gamma},t)=\frac{a}{m_e}\sum_{l=0}^{\infty}h_\ell P_\ell(\cos\gamma)$$

And the surface load love numbers k_ℓ & h_ℓ in turn have expansions :

$$k_\ell=k_\ell^E+\sum_{k=1}^{K}r_j^{\ell\prime}e^{-s_j^\ell t}$$
$$h_\ell=h_\ell^E+\sum_{k=1}^{K}r_j^{\ell}e^{-s_j^\ell t}$$

ROTATIONAL FEEDBACK IN THE SEALEVEL EQUATION

Because a change in rotational state is accompanied by a change in centrifugal potential and because sea level (msl) is constrained to lie on an equipotential, a change in rotational state will clearly induce a change in sea level.

∴ A Modified Sea Level Equation

$$S(\theta,\lambda,t)=C(\theta,\lambda,t)\left[\int_{-\infty}^{t}dt'\int_{\Omega e}\int d\Omega'\left\{L(\theta',\lambda',t')G_\phi^L(\gamma,t-t')+\psi^R(\theta',\lambda',t')G_\phi^T(\gamma,t-t')\right\}+\frac{\Delta\Phi(t)}{g}\right]$$

Where, to first order in perturbation theory

$$\psi^R=\psi^{00}+\sum_{m=-1}^{+1}\psi_{2m}Y_{2m}(\theta,\lambda)$$
$$\psi_{00}=+\frac{2}{3}\omega_3\Omega_0 a^2$$
$$\psi_{20}=-\frac{1}{3}\omega_3\Omega_0 a^2\sqrt{4/5}$$
$$\psi_{21}=+(\omega_1-i\omega_2)(\Omega_0 a^2/2)\sqrt{2/15}$$
$$\psi_{2-1}=-(\omega_1+i\omega_2)(\Omega_0 a^2/2)\sqrt{2/15}$$

Rot in S, Dahlen 1976
Milne & Mit. 1997,
Peltier 1998

Data for Rot in S,
Peltier 2002

Rot in Geoid,
eg Peltier et al
2012

Holocene relative sea level histories

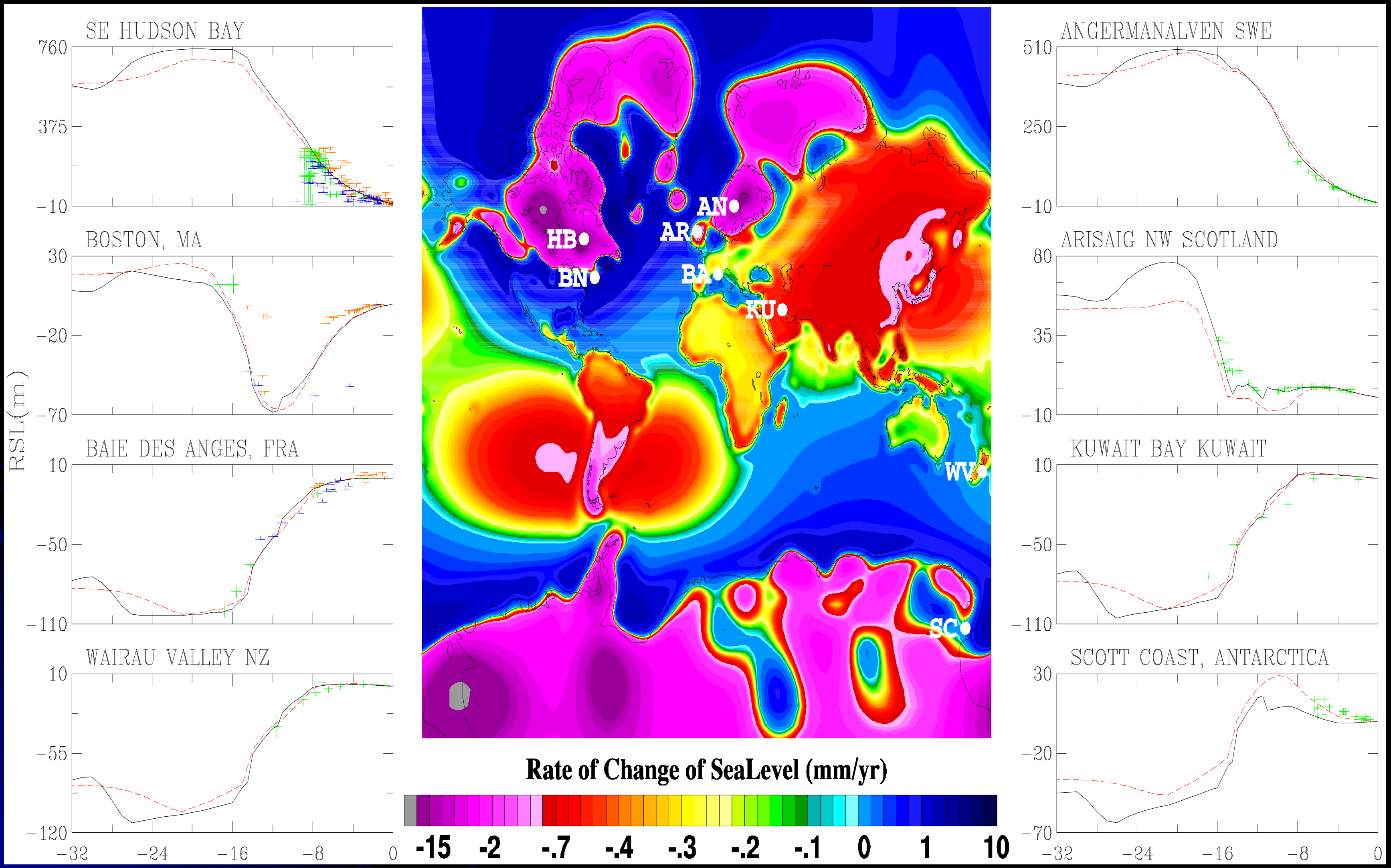

Northern hemisphere paleotopographies

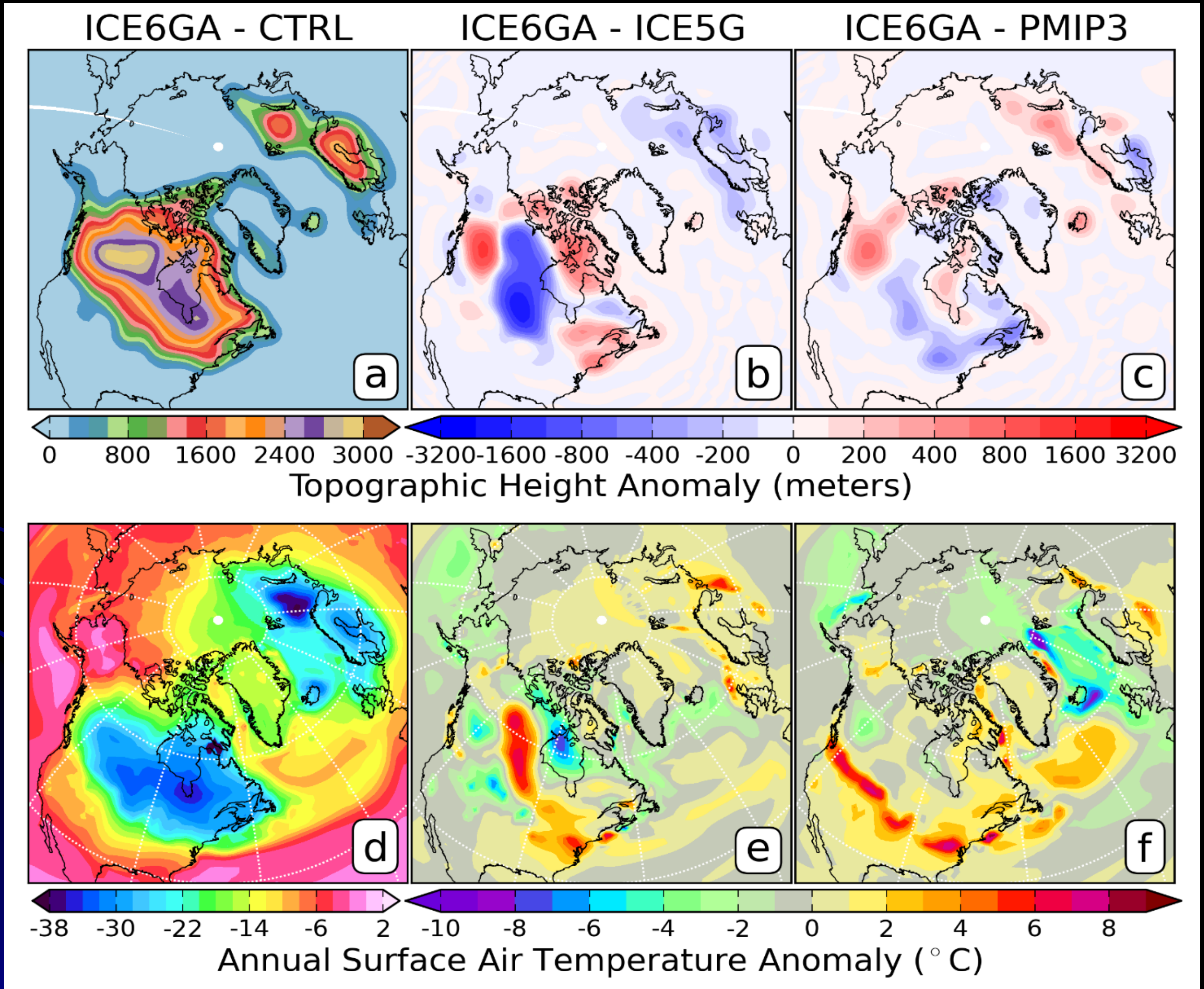

From Vettoretti & P GRL, 2013

The vertical turbulent diffusivities of mass and momentum in the global oceans: Existing parameterizations

Parameterizations of these diffusivities are evolving rapidly: We show that the D-O oscillation process is small scale mixing dependent and therefor may be invoked to help constrain such parameterizations

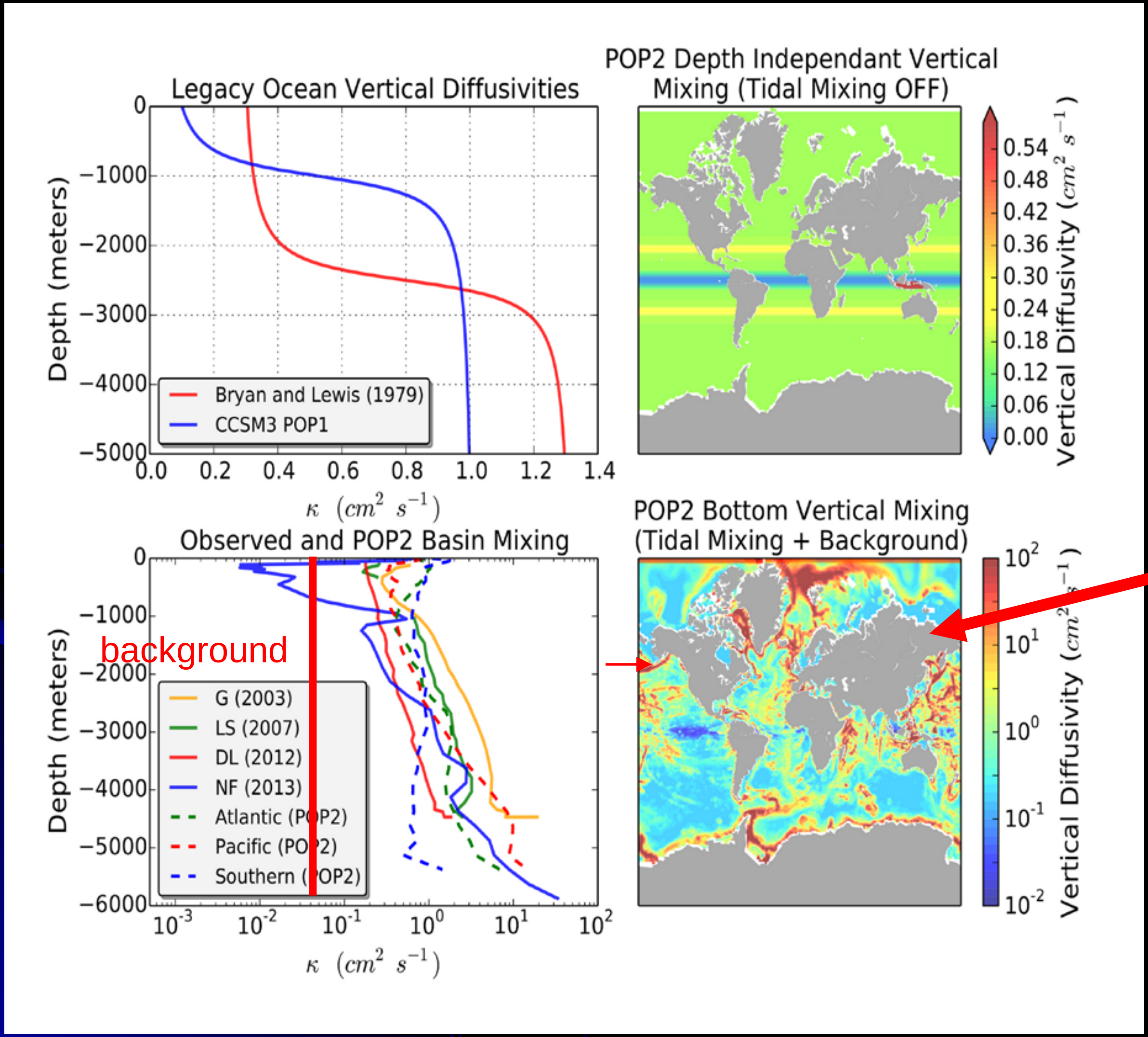

Our interest is in the question of the dependence of coupled climate model predictions of the D-O oscillation upon the parameterization of the vertical diapycnal diffusion of mass

A modern diffusivity map based upon the assumption that this turbulent process is controlled by dissipation of the "internal tide "

From P & Vettoretti GRL, 2014

Validation of a model of global barotropic tides against TOPEX-Poseidon satellite altimetry: the modern tidal regime

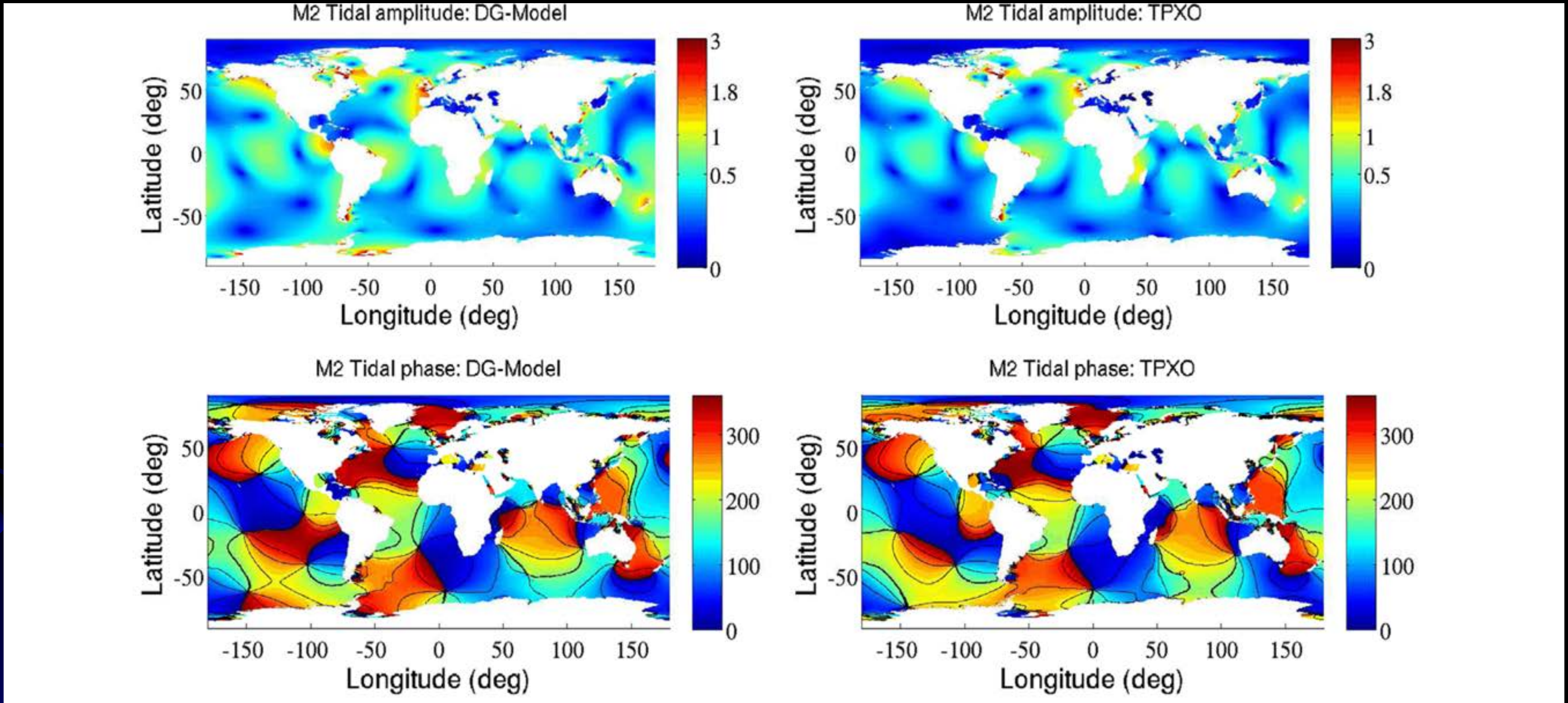

Fig. 10. The global picture of the M_2 tidal amplitude (top) and phase (bottom) from Left: DG-model with *N*¼3 and Right: TPXO 7.2 dataset on a a grid with about 60 km resolution in deep ocean and 7.5 km around the global coasts.

A discontinuous Galerkin model: Salehipour, Stuhne and P, Oc Mod, 2012

Simulated tidal amplitude and dissipation between LGM and Modern

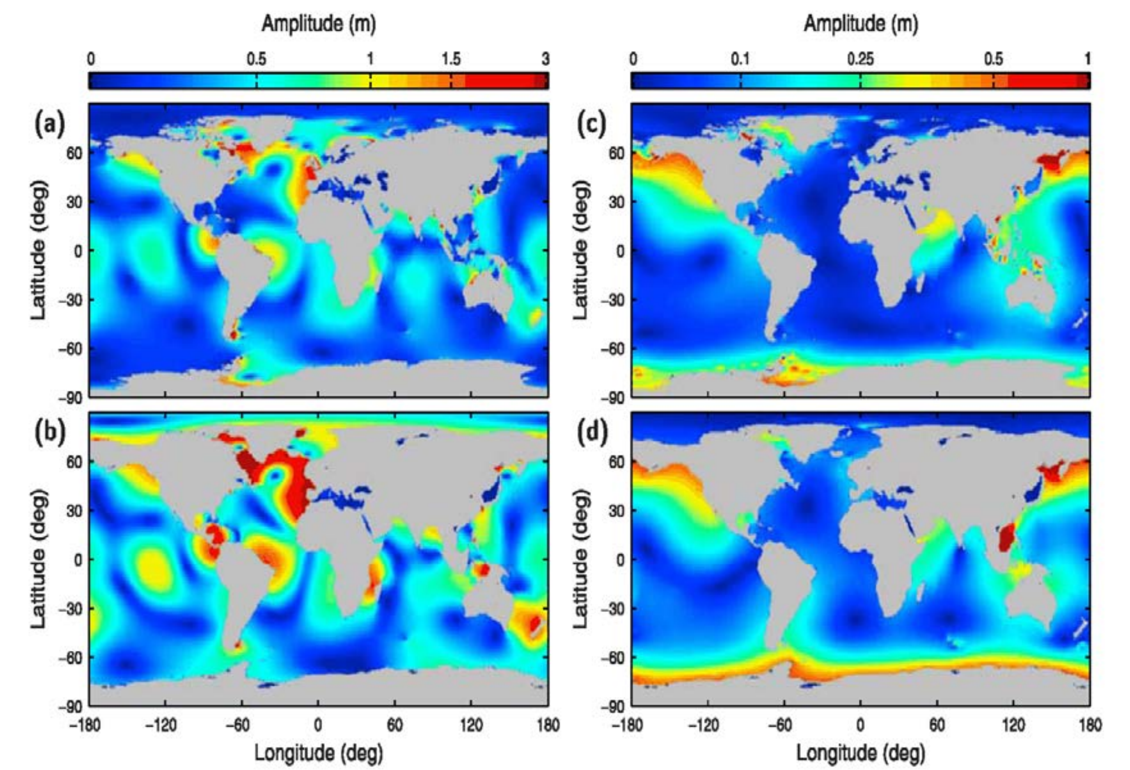

Figure 2. Modeled tidal amplitudes: (a) M_2, present-day; (b) M_2, LGM; (c) K_1, present-day; (d) K_1, LGM.

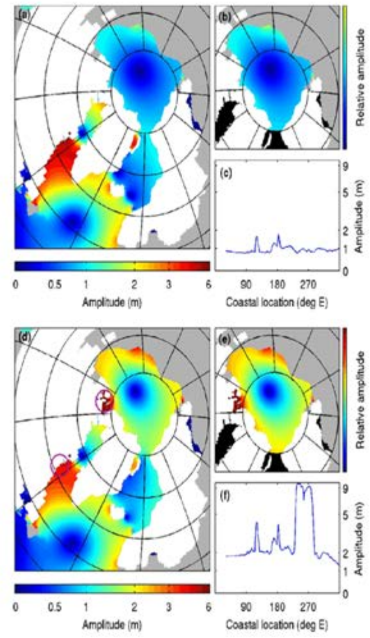

Figure 3. (a) Modeled LGM M_2 tidal amplitude. (b) Relative amplitude of the normal mode with frequency $1.403 \times 10^{-4}\ s^{-1}$. The oceans excluded from the normal-mode calculation are black. (c) Amplitude of the modeled M_2 tide along the Arctic coastline. The longitudes given are approximate, since the coastline winds back on itself in some places. (d) Modeled LGM M_2 tidal amplitude with the QEI surrounded by water. The purple circles show positions of two sources of ice-rafted debris. (e) Relative amplitude of the normal mode with frequency $1.332 \times 10^{-4}\ s^{-1}$. (f) Amplitude of the modeled M_2 tide along the Arctic coastline.

From Griffiths & P, GRL (2008) and J Climate (2009).

GRIP and NGRIP Summit Greenland Ice Cores: Relaxation oscillations of the global ocean circulation?

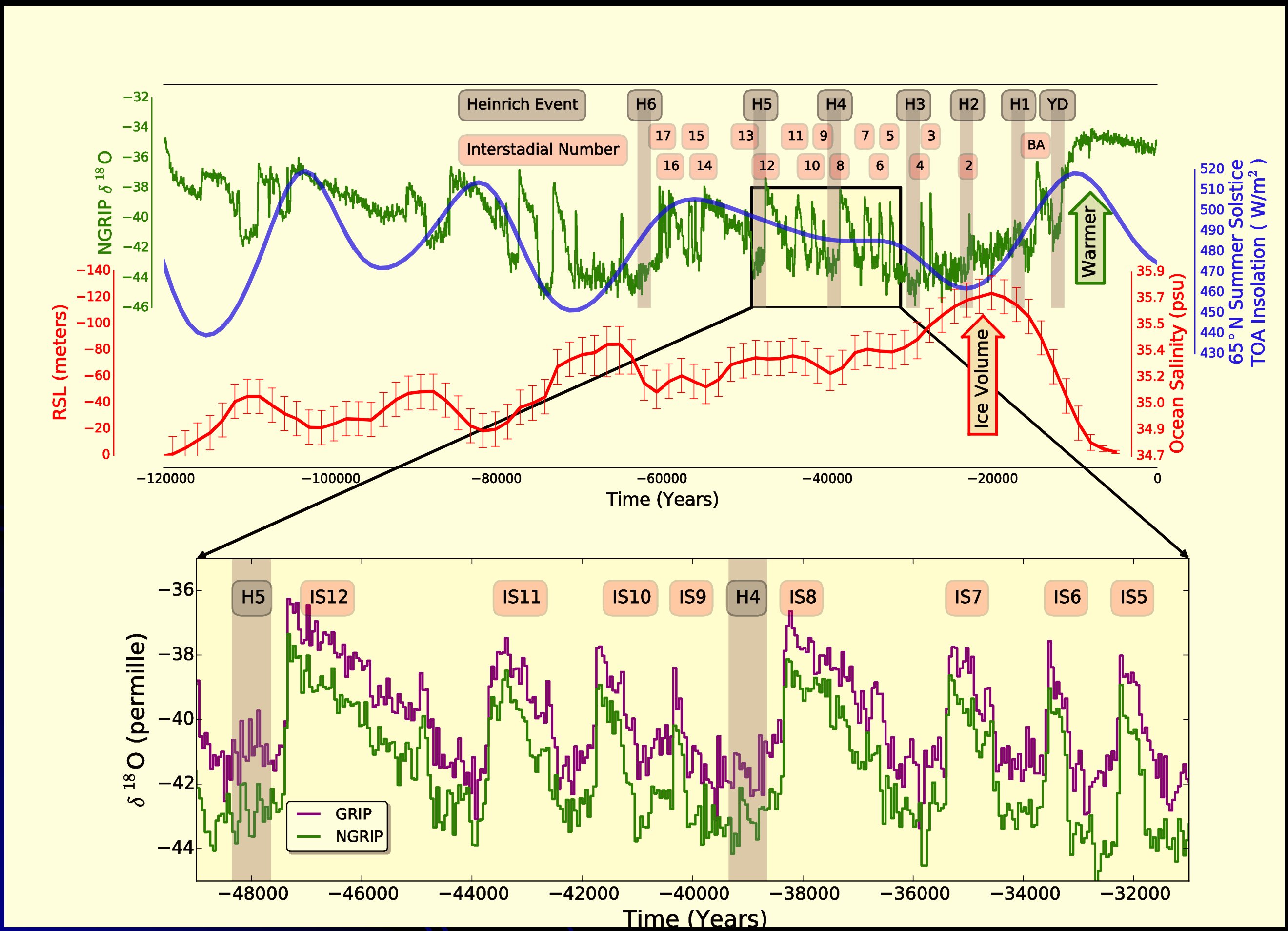

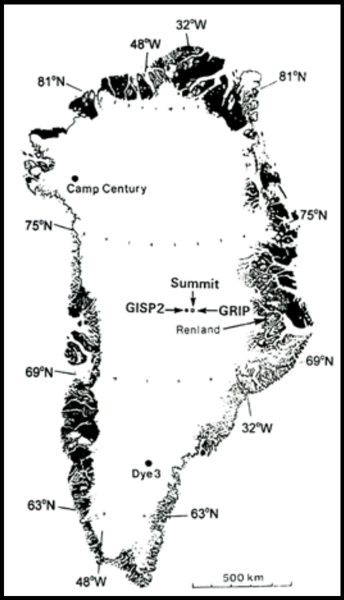

The oxygen isotopic ratio measured in ice is a measure of the temperature of the air from which precip. is derived.

Heinrich events (H) correspond to episodes during which intense instabilities occur on the eastern flank of the Laurentide ice sheet.

Initial conditions for the integration of the NCAR CESM1 model under glacial boundary conditions

- Thermal state of the oceans=modern
- Dynamical state of the oceans=at rest
- Salinity state of the oceans=+1 psu above modern
- Atmospheric trace gases from Vostok, eg pCO_2=200 ppmv
- Orbital solar insolation = 21,000 years before present

We explore coupled climate model sensitivity to the mixing parameterization

- Constant pelagic value
- CCSM3 value
- CESM1 modern tidal mixing parameterization, a sensitivity test

The Annual Cycle of Sea Ice Variability Under Both Modern and Ice-Age Conditions

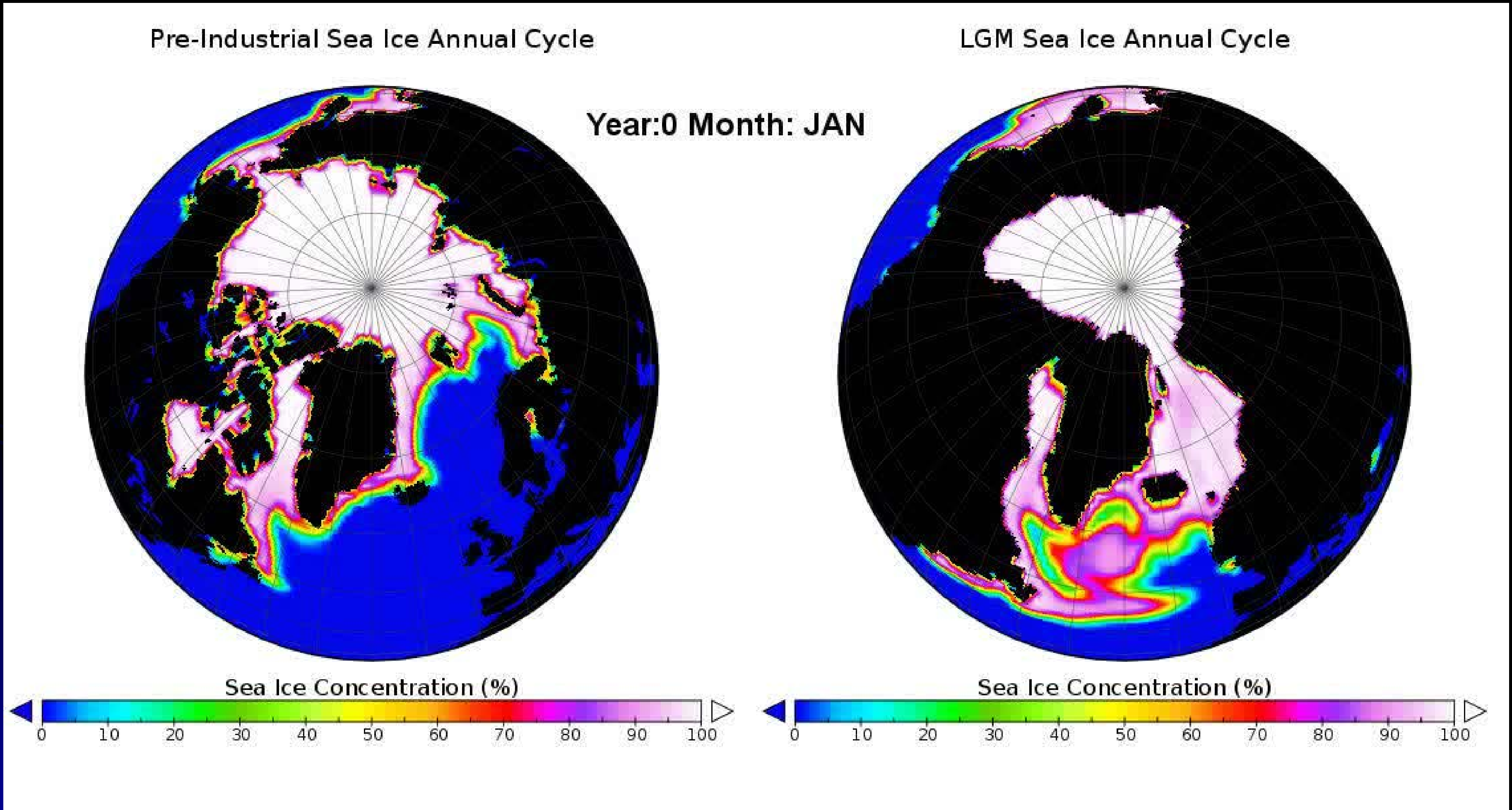

First global climate model simulation of the Dansgaard-Oeschger oscillation: A “kicked” salt oscillator in the glacial Atlantic Ocean

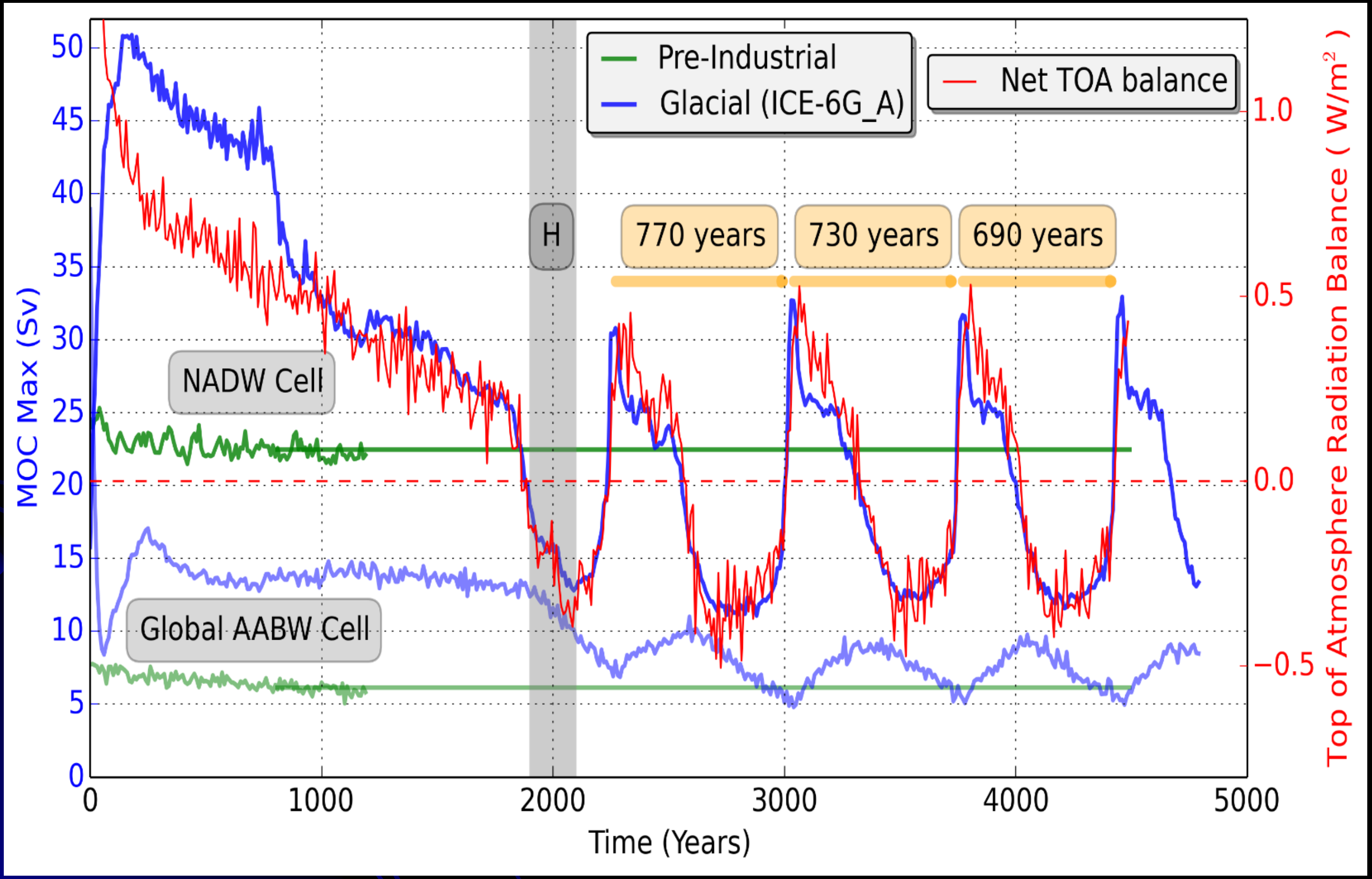

From P&Vettoretti GRL, 2014

Kappa= constant

Note the somewhat reduced period of the MOC oscillation compared with Summit data

A comparison of the oscillation for two different choices of diapycnal diffusivity

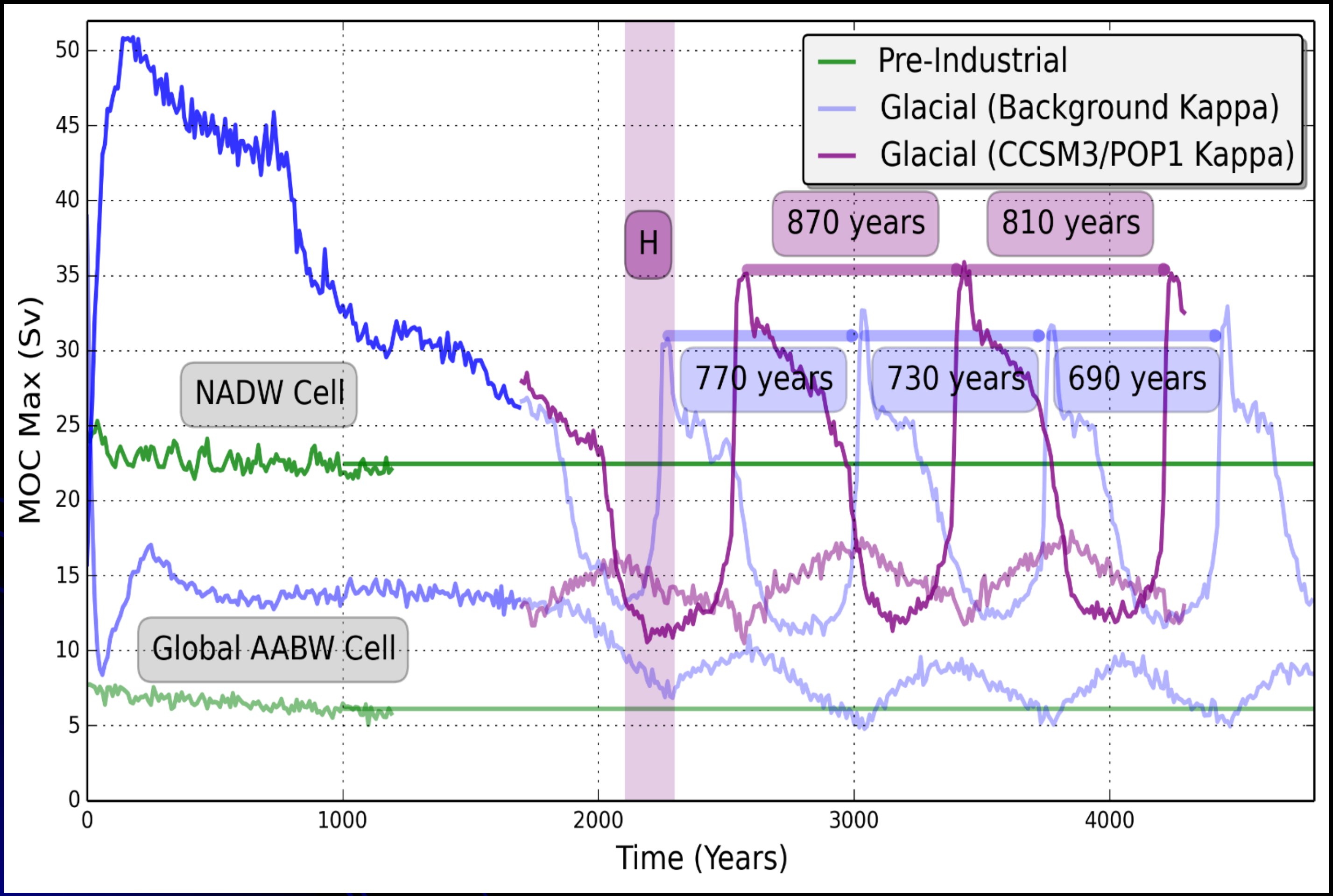

From P & Vettoretti GRL, 2014

Kappa = CCSM3

Conclusion: the strength of the MOC depends strongly on turbulent diapycnal diffusivity

North-south sections through the zonally averaged salinity field & D-O time series: A "kicked" salt oscillator in the Atlantic

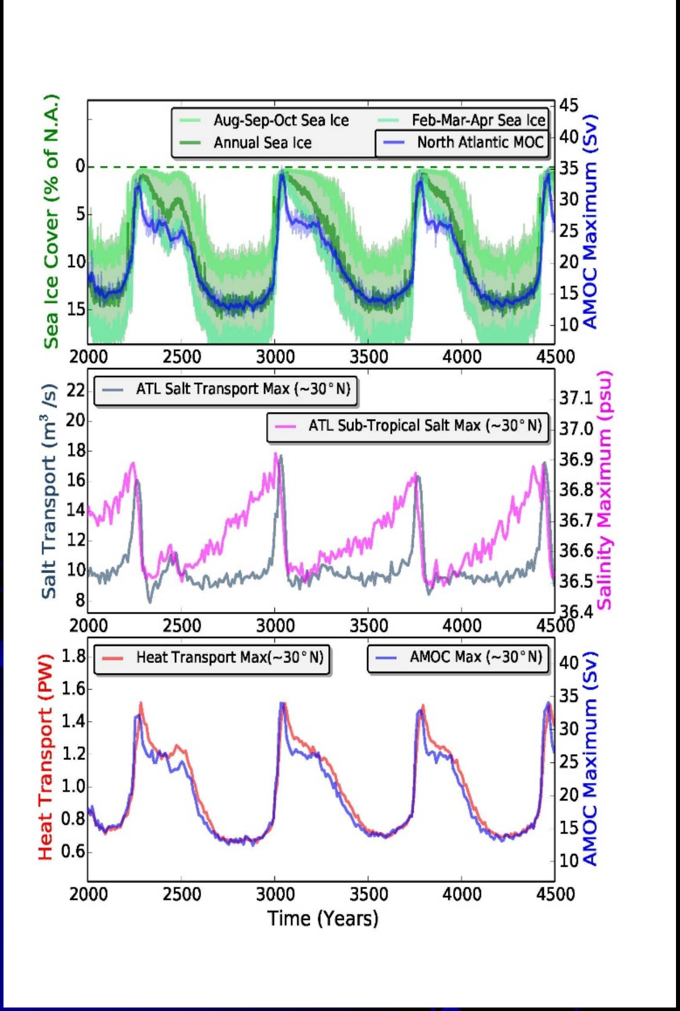

D-O Oscillation time series

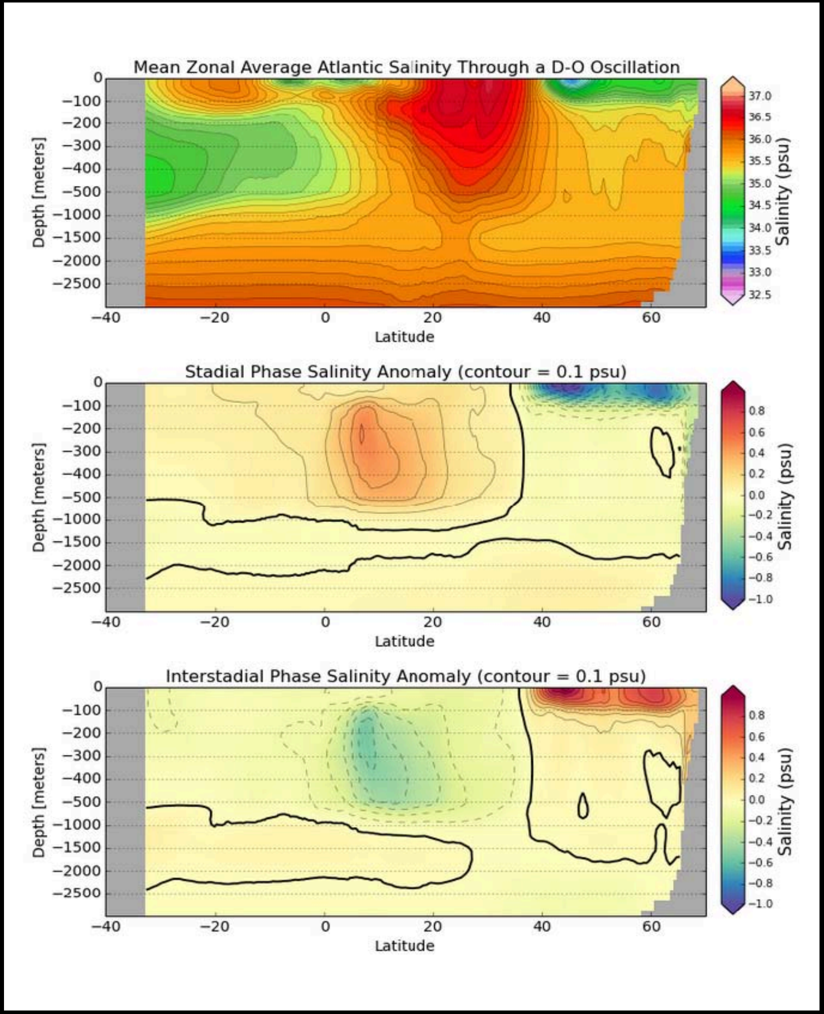

Zonal And D-O mean

Stadial

Inter-stadial

From P & Vettoretti, 2014

The modeled relaxation oscillations fit the polar ice core inferred SAT data well—but not with tidal mixing turned on: For the simpler modes we have-

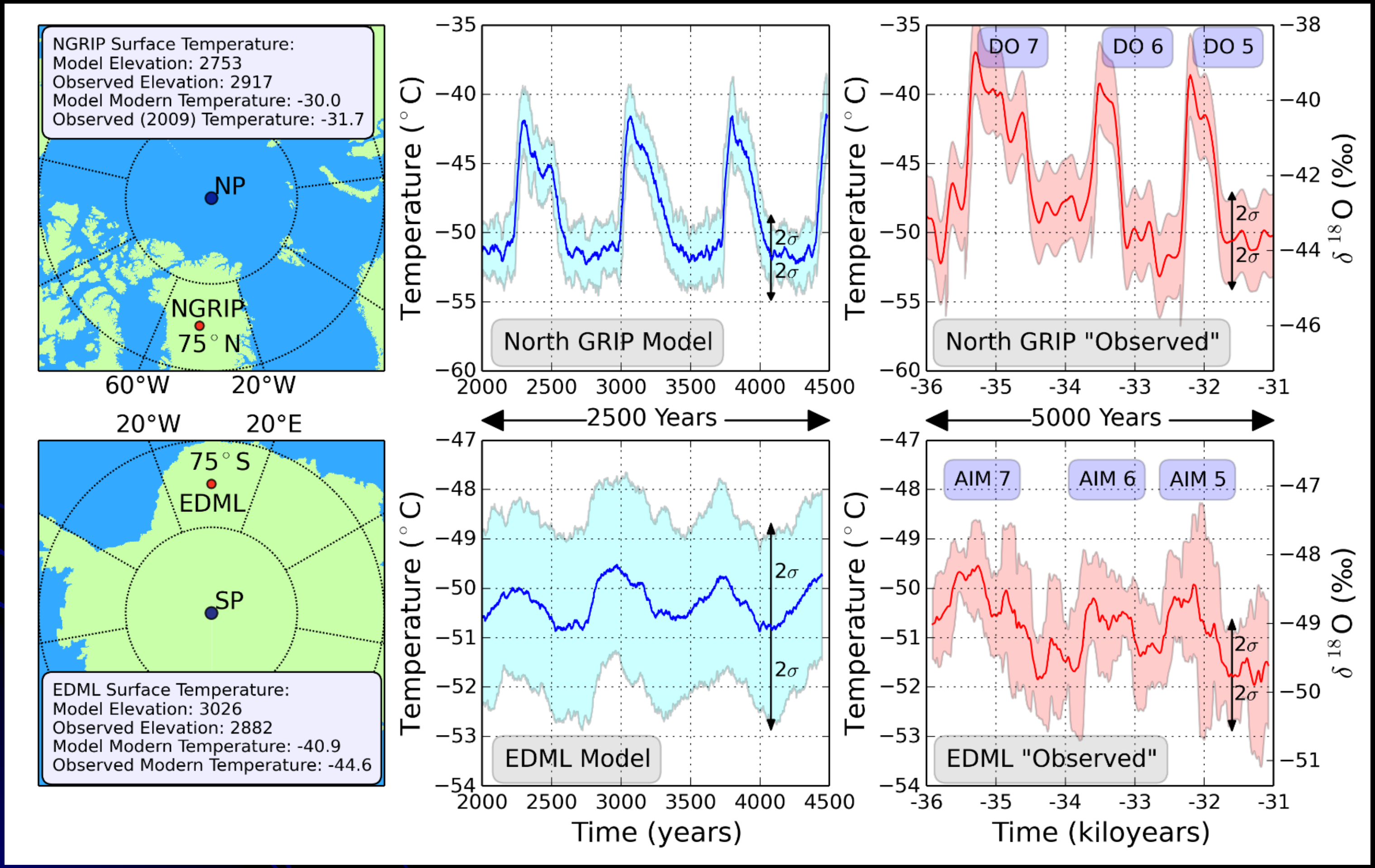

Ice provides the memory of the climate variability associated with the presence of ice

Physical origins of the fast timescale aspect of the relaxation oscillation: a sub-sea ice thermohaline instability opens a super-polynya

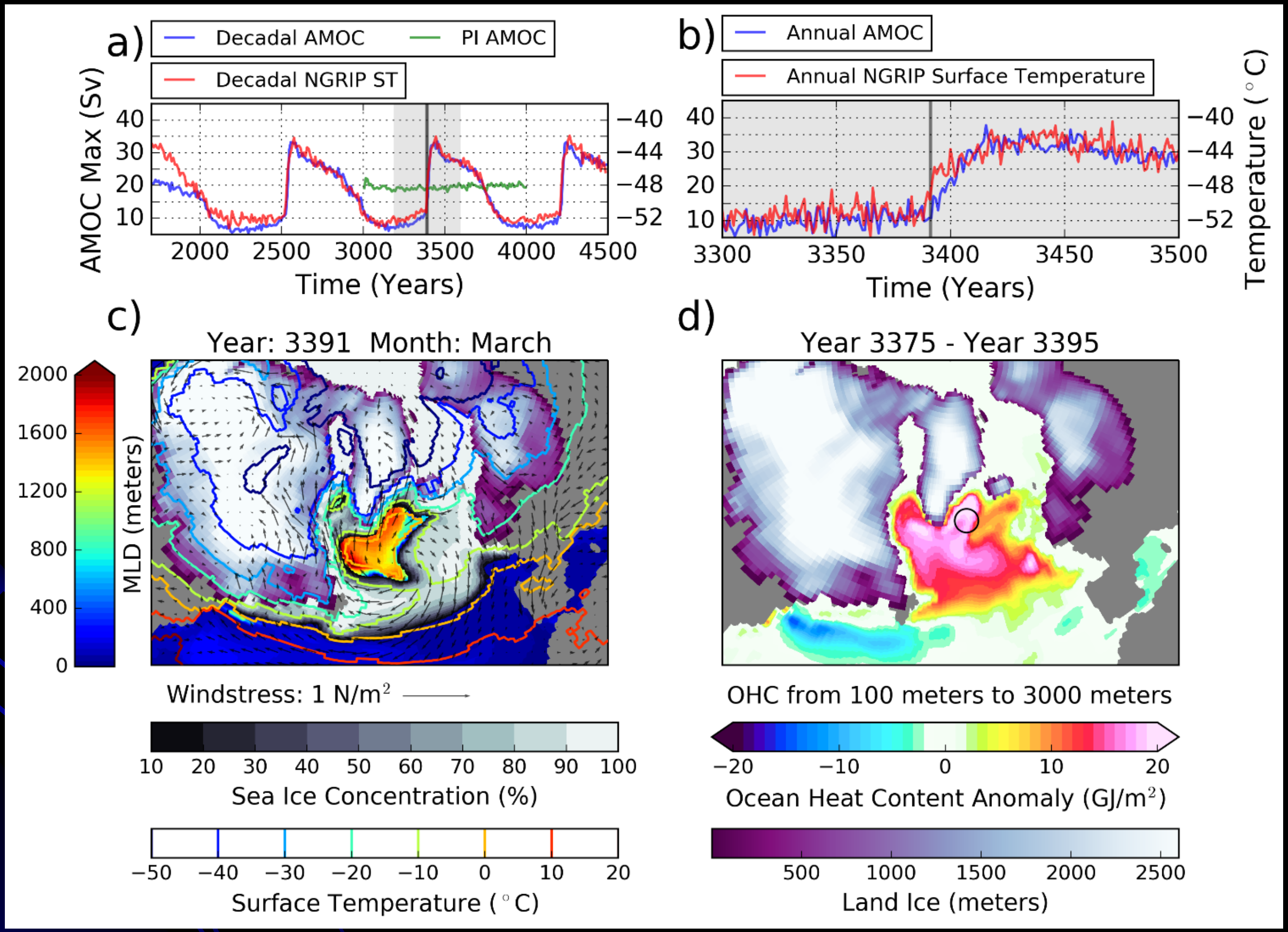

From Vettoretti and P, GRL, 2016

Water mass transformation during polynya formation by convective destabilization of the water column

Before transition

After transition

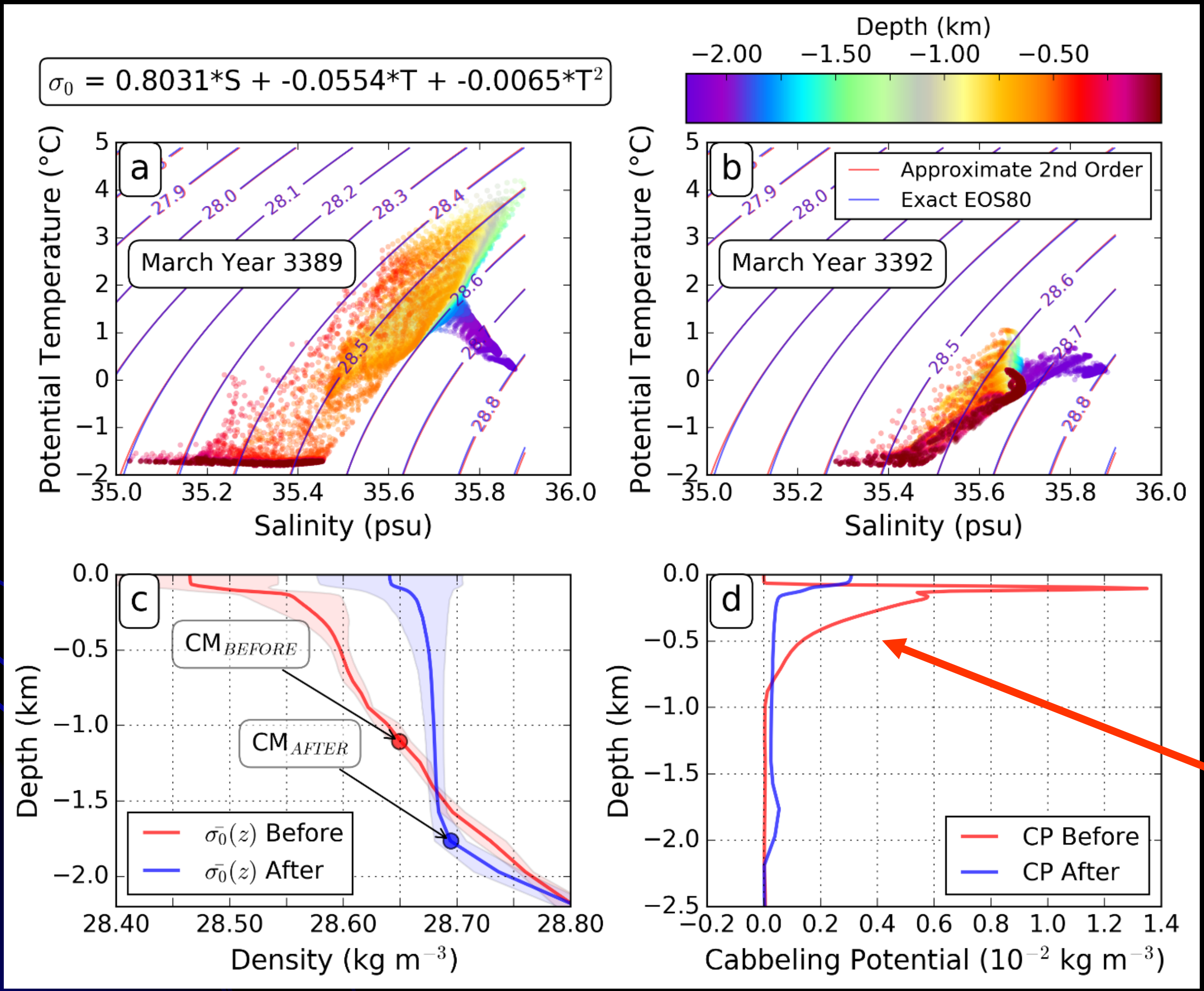

Note the drop in the COM

Cabelling potential

Water column below the polynya before and after its formation

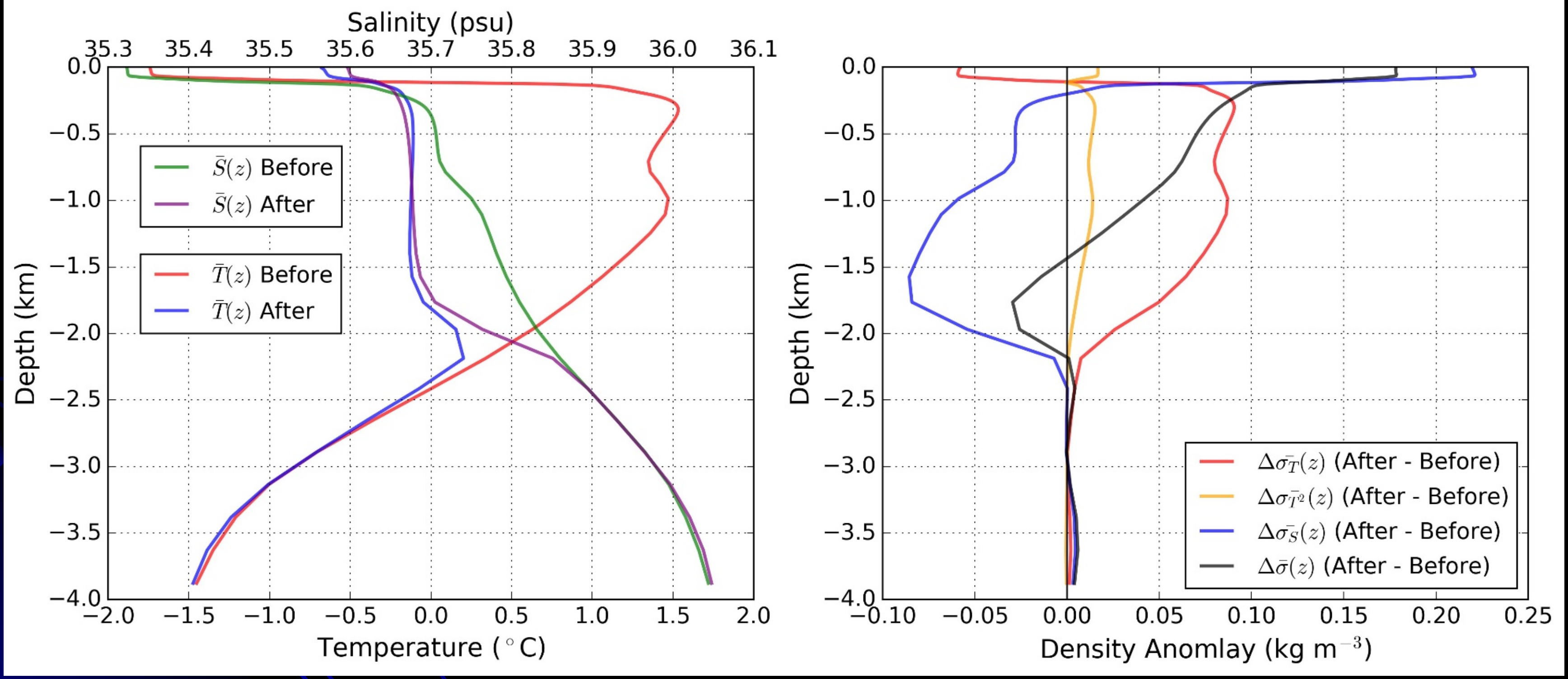

The Arctic Component of the Relaxation Oscillation: Basin Averaged Data

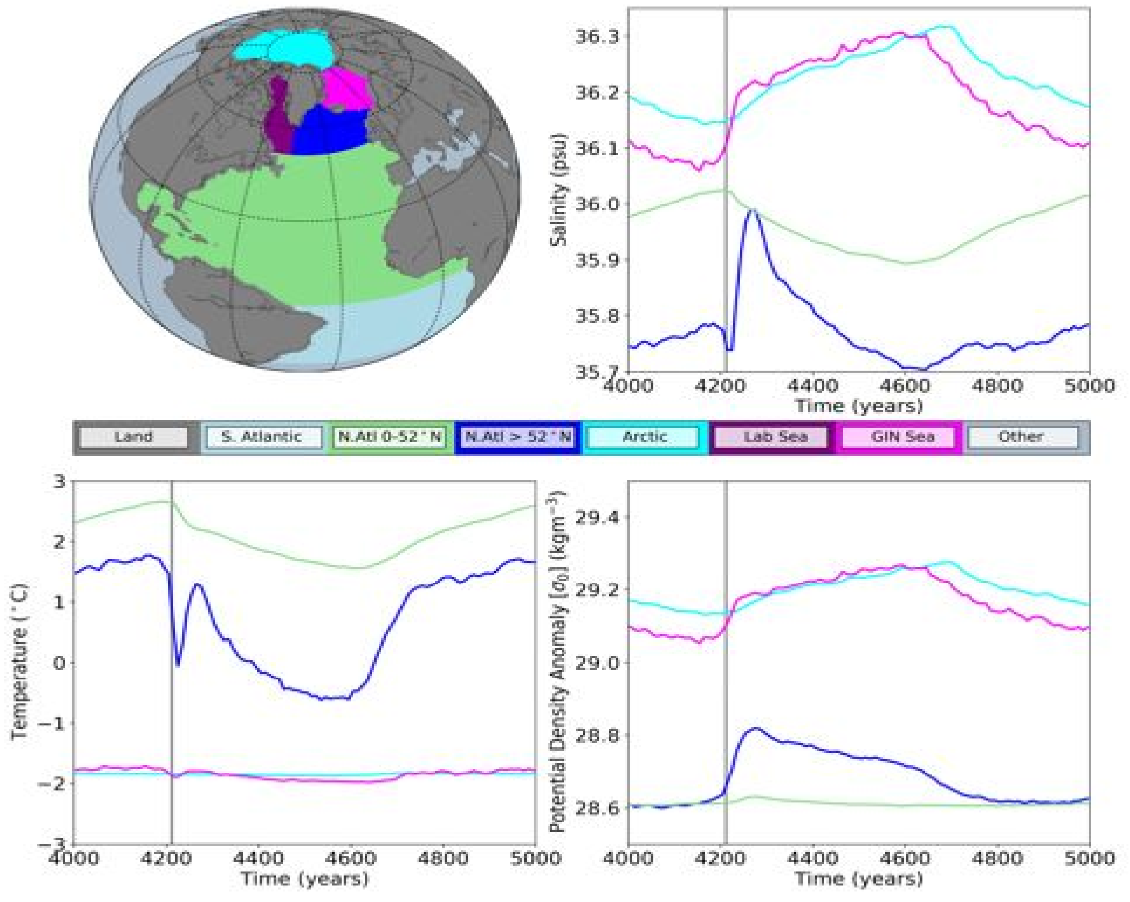

Figure 2: a) Ocean regions described in the paper: Arctic (cyan), GIN seas (magenta), Labrador Sea (purple), North Atlantic greater than 52°N (blue), North Atlantic between the equator and 52°N latitude (green), and the South Atlantic (light blue). Timeseries of North Atlantic and Polar b) salinity, c) temperature, and d) potential density anomaly referenced to the surface. The timeseries are color coded according to the regions in a).

From Vettoretti and P, J Climate, submitted, 2017.

Water mass properties on a section across the Denmark Strait into the Irminger Sea

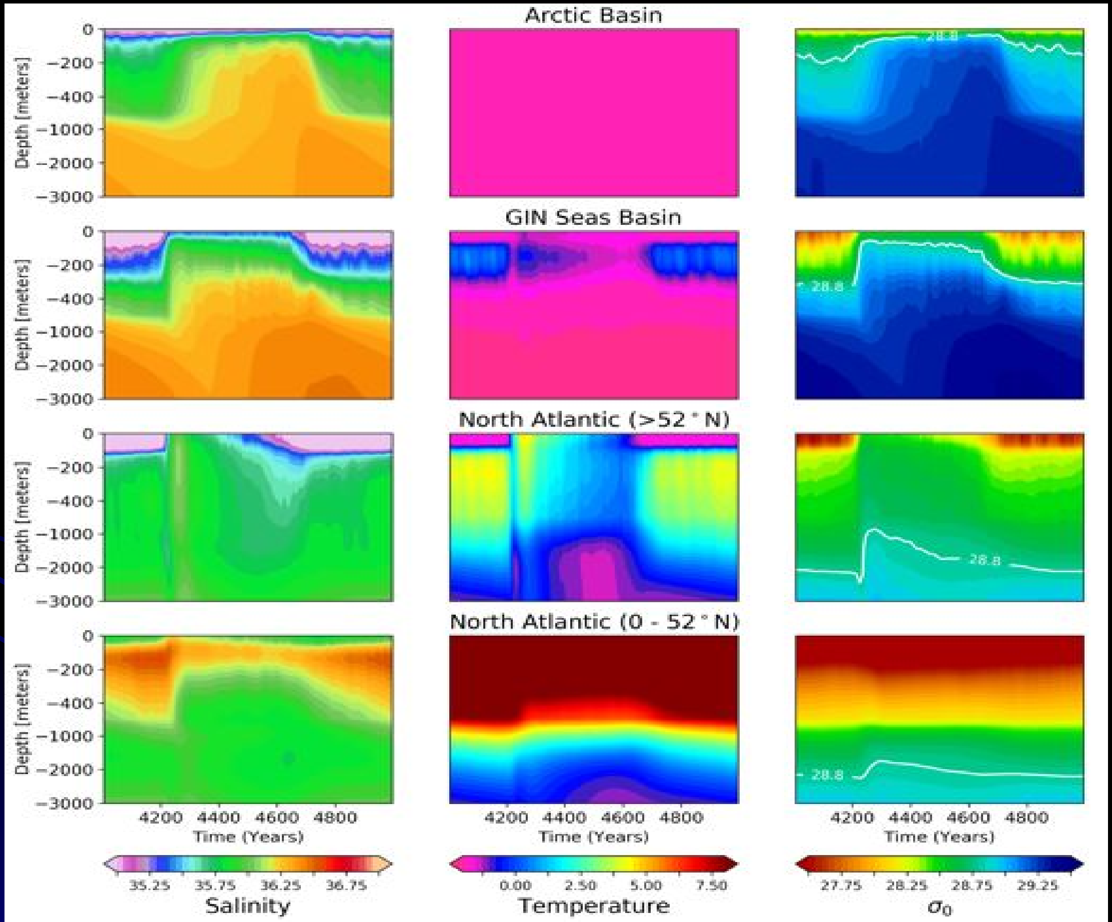

Figure 3: Timeseries of the mean basin salinity (psu), temperature (°C) and potential density anomaly referenced to the surface (kg m^{-3}). The four ocean regions correspond to the basins from Figure 1a. The σ_0=28.8 kg m^{-3} isopycnal is displayed in white to indicate the approximate vertical location of dense waters that originate from the Arctic.

From Vettoretti and P, J Climate, 2017, submitted

The salinity above the pycnocline increases, the vertical salinity gradient relaxes and thermohaline convective turbulence commences

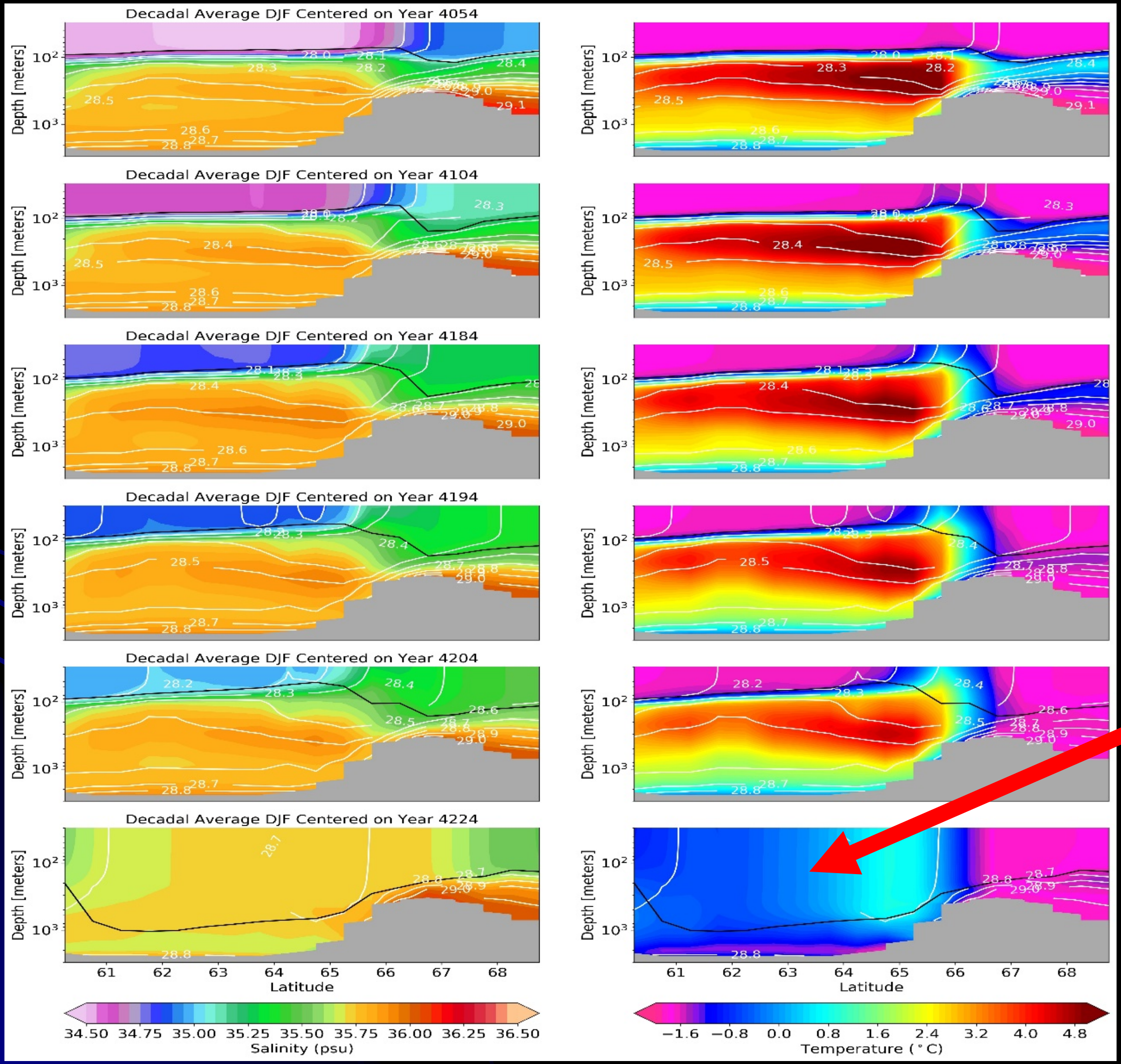

Sections across the Denmark Strait Sill into the Irminger Sea

Deep turbulent mixing commences

Summary

- The Dansgaard-Oeschger oscillation has been explained in terms of nonlinear free relaxation oscillation of the global overturning circulation.
- It is sensitive to the detailed structure of diapycnal diffusivity
- The fact that a modern coupled atmosphere-ocean climate model is able to explain this phenomenon is a major success demonstrating robustness well removed from the parameter space in which the model has been tuned
- Existing models of the variation of kappa throughout the volume of the ocean destroy the fit to the otherwise excellent representation of this phenomenon using conventional and much simpler models of kappa